Robust And Optimal Opportunistic Scheduling For Downlink 2-Flow Network Coding With Varying Channel Quality and Rate Adaptation (New Simulation Figures)

Wei-Cheng Kuo, Chih-Chun Wang {wkuo, chihw}@purdue.edu
School of Electrical and Computer Engineering, Purdue University, USA

arXiv:1606.04205v1 [cs.NI] 14 Jun 2016

***Abstract*—This paper considers the downlink traffic from a base station to two different clients. When assuming infinite backlog, it is known that *inter-session* network coding (INC) can significantly increase the throughput. However, the corresponding scheduling solution (when assuming dynamic arrivals instead and requiring bounded delay) is still nascent.**

For the 2-flow downlink scenario, we propose the first opportunistic INC + scheduling solution that is provably optimal for time-varying channels, i.e., the corresponding stability region matches the optimal Shannon capacity. Specifically, we first introduce a new *binary INC* operation, which is distinctly different from the traditional wisdom of XORing two overheard packets. We then develop a *queue-length-based* scheduling scheme and prove that it, with the help of the new INC operation, achieves the optimal stability region with time-varying channel quality. The proposed algorithm is later generalized to include the capability of rate adaptation. Simulation results show that it again achieves the optimal throughput with rate adaptation. A byproduct of our results is a scheduling scheme for stochastic processing networks (SPNs) with *random departure*, which relaxes the assumption of *deterministic departure* in the existing results.

I. Introduction

Since 2000, network coding (NC) has emerged as a promising technique in communication networks. [1] shows that linear intra-session NC achieves the min-cut/max-flow capacity of single-session multi-cast networks. The natural connection between intra-session NC and the *maximum flow* allows the use of back-pressure (BP) algorithms to stabilize intra-session NC traffic, see [2] and the references therein.

However, when there are multiple coexisting sessions, the benefits of *inter-session* NC (INC) are not fully utilized [3], [4]. The COPE architecture [5] demonstrated that a simple INC scheme can provide 40%–200% throughput improvement in a testbed environment. Several analytical attempts have been made to characterize the INC capacity for various small network topologies [6]–[8].

However, unlike the case of intra-session NC, there is no direct analogy from INC to the commodity flow. As a result, it is much more challenging to derive BP-based scheduling for INC traffic. We use the following example to illustrate this point. Consider a single source s and two destinations d_1 and d_2. Source s would like to send to d_1 the X_i packets, $i = 1, 2, \cdots$; and send to d_2 the Y_j packets, $j = 1, 2, \cdots$. The simplest INC scheme consists of three operations. OP1: Send uncodedly those X_i that have not been heard by any of $\{d_1, d_2\}$. OP2: Send uncodedly those Y_j that have not been heard by any of $\{d_1, d_2\}$. OP3: Send a linear sum $[X_i + Y_j]$ where X_i has been overheard by d_2 but not by d_1 and Y_j has been overheard by d_1 but not by d_2. For future reference, we denote OP1 to OP3 by NON-CODING-1, NON-CODING-2, and CLASSIC-XOR, respectively.

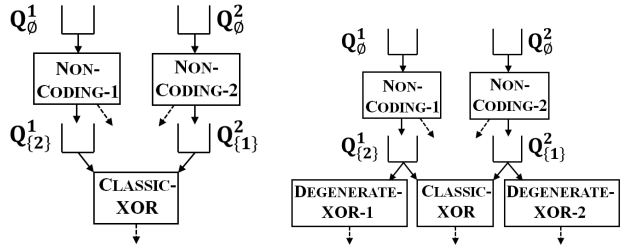

(a) INC using only 3 operations (b) INC using only 5 operations

Fig. 1. The virtual networks of two INC schemes.

OP1 to OP3 can also be represented by the virtual network (vr-network) in Fig. 1(a). Namely, any newly arrived X_i and Y_j virtual packets[1] (vr-packets) that have not been heard by any of $\{d_1, d_2\}$ are stored in queues $Q^1_\emptyset$ and $Q^2_\emptyset$, respectively. The superscript $k \in \{1, 2\}$ indicates that the queue is for the session-k packets. The subscript $\emptyset$ indicates that those packets have not been heard by any of $\{d_1, d_2\}$. NON-CODING-1 then takes one X_i vr-packet from $Q^1_\emptyset$ and send it uncodedly. If such X_i is heard by d_1, then the vr-packet leaves the vr-network, which is described by the dotted arrow emanating from the NON-CODING-1 block. If X_i is overheard by d_2 but not d_1, then we place it in queue $Q^1_{\{2\}}$, the queue for the overheard session-1 packets. NON-CODING-2 in Fig. 1(a) can be interpreted symmetrically. CLASSIC-XOR operation takes an X_i from $Q^1_{\{2\}}$ and a Y_j from $Q^2_{\{1\}}$ and sends $[X_i + Y_j]$. If d_1 receives $[X_i + Y_j]$, then X_i is removed from $Q^1_{\{2\}}$ and leaves the vr-network. If d_2 receives $[X_i + Y_j]$, then Y_j is removed from $Q^2_{\{1\}}$ and leaves the vr-network.

This work was supported in parts by NSF grants ECCS-1407603, CCF-0845968 and CCF-1422997. Part of the results was presented in 2014 INFOCOM.

[1]We denote the packets (jobs) inside the vr-network by "virtual packets."

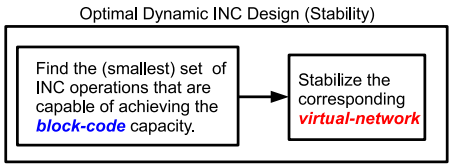
Optimal Dynamic INC Design (Stability)
Find the (smallest) set of INC operations that are capable of achieving the block-code capacity.
Stabilize the corresponding virtual-network

Fig. 2. The two components of optimal dynamic INC design.

It is known [9] that with dynamic packet arrivals, any INC scheme that (i) uses only these three operations and (ii) attains bounded decoding delay with rates (R_1, R_2) can be converted to a scheduling solution that stabilizes the vr-network with rates (R_1, R_2), and vice versa. *The INC design problem is thus converted to a vr-network scheduling problem.* To distinguish the above INC design for dynamical arrivals (the concept of stability regions) from the INC design assuming infinite backlog and decoding delay (the concept of the Shannon capacity), we term the former *the dynamic INC* design problem and the latter *the block-code INC* design problem.

The above vr-network representation also allows us to divide the optimal dynamic INC design problem into solving the following two major challenges separately. **Challenge 1**: The example in Fig. 1(a) focuses on dynamic INC schemes using only 3 possible operations. Obviously, the more INC operations one can choose from, the larger the degree of design freedom, and the higher the achievable throughput. *The goal is thus to find a (small) finite set of INC operations that can provably maximize the "block-code" achievable throughput.* **Challenge 2**: Suppose that we have found a set of INC operations that is capable of achieving the block-code capacity. However, it does not mean that such a set of INC operations will automatically lead to an optimal dynamic INC design since we still need to consider the delay/stability requirements. Specifically, once the best set of INC operations is decided, we can derive the corresponding vr-network as discussed in the previous paragraphs. *The goal then becomes to devise a stabilizing scheduling policy for the vr-network, which leads to an equivalent representation of the optimal dynamic INC solution.* See Fig. 2 for the illustration of these two tasks.

Both tasks turn out to be highly non-trivial and optimal dynamic INC solution [6], [9], [10] has been designed only for the scenario of fixed channel quality. Specifically, [11] answers Challenge 1 and shows that for fixed channel quality, the 3 INC operations in Fig. 1(a) plus 2 additional DEGENERATE-XOR operations, see Fig. 1(b) and Section III-A, can achieve the block-code INC capacity. One difficulty of resolving Challenge 2 is that an INC operation may involve multiple queues simultaneously, e.g., CLASSIC-XOR can only be scheduled when *both* $Q^1_{\{2\}}$ and $Q^2_{\{1\}}$ are non-empty. This is in sharp contrast with the traditional BP solutions [12], [13] in which each queue can act independently.[2] For the vr-network in Fig. 1(b), [6] circumvents this problem by designing a fixed priority rule that gives strict precedence to the CLASSIC-XOR operation. Alternatively, [9] derives a BP scheduling scheme by noticing that the vr-network in Fig. 1(b) can be decoupled into two vr-subnetworks (one for each data session) so that the queues in each of the vr-subnetworks can be activated independently and the traditional BP results follow.

However, the channel quality varies over time for practical wireless downlink scenarios. Therefore, one should opportunistically choose the most favorable users as receivers, the so-called *opportunistic scheduling* technique. Recently [15] shows that when allowing opportunistic coding+scheduling for time-varying channels, the 5 operations in Fig. 1(b) no longer achieve the block-code capacity. The existing dynamic INC design in [6], [9] are thus strictly suboptimal for time-varying channels since they are based on a suboptimal set of INC operations (recall Fig. 2).

This paper also considers *rate adaptation*. When NC is not allowed, the existing practical schemes simply chooses a reliable modulation-and-coding-scheme (MCS) (e.g. drop rate less than 0.1) with the highest transmission rate. However, when NC is allowed, it is not clear how to perform rate adaptation. The reason is that while using a high-rate MCS can directly increase the point-to-point throughput, using a low-rate MCS increases the chance of overhearing and thus maximizes the opportunity of performing CLASSIC-XOR that combines overheard packets to enhance throughput. How to balance the usage of high-rate and low-rate MCSs remained a critical and open problem in NC design.

This work proposes new optimal dynamic INC designs for 2-flow downlink traffic with time-varying packet erasure channels (PECs) and with rate adaptation. Our detailed contributions are summarized as follows.

Contribution 1: We introduce a new pair of INC operations such that (i) The underlying concept is distinctly different from the traditional wisdom of XORing two overheard packets; (ii) The overall scheme uses only the low-complexity binary XOR operation; and (iii) We prove that the new set of INC operations is capable of achieving the block-code-based Shannon capacity for the setting of time-varying PECs.

Contribution 2: The new INC operations lead to a new vr-network that is different from Fig. 1(b) and the existing "*vr-network decoupling + BP*" approach in [9] no longer holds. To answer Challenge 2, we generalize the results of Stochastic Processing Networks (SPNs) [16], [17] and apply it to the new vr-network. The end result is an opportunistic, dynamic INC solution that is *queue-length-based* and can robustly achieve the optimal stability region of time-varying PECs.

Contribution 3: The proposed solution is also generalized for rate-adaptation. In simulations, our scheme can opportunistically and optimally choose the MCS of each packet transmission while achieving the optimal stability region, i.e., equal to the Shannon capacity. This new result is the first capacity-achieving INC solution which considers jointly coding, scheduling, and rate adaptation for 1-base-station-2-session-client scenario.

Contribution 4: A byproduct of our results is a scheduling scheme for SPNs with *random departure* instead of *deterministic departure*, which relaxes a major limitation of the existing SPN model. The results could thus further broaden the

[2] A critical assumption in [Section II C.1 [14]] is that if two queues Q_1 and Q_2 can be *activated* at the same time, then we can also choose to activate only one of the queues if desired. This is not the case in the vr-network. E.g., CLASSIC-XOR activates both $Q^1_{\{2\}}$ and $Q^2_{\{1\}}$ but no coding operation in Fig. 1(a) activates only one of $Q^1_{\{2\}}$ and $Q^2_{\{1\}}$.

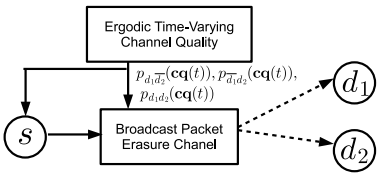

Fig. 3. The time-varying broadcast packet erasure channel.

applications of SPN scheduling to other real-world scenarios.

Organization of this work: Section II defines the optimal stability region when allowing arbitrary NC operations. Sections III first explains the sub-optimality of existing INC operations and then introduce two new XOR-based operations that are capable of achieving the optimal Shannon capacity. The corresponding vr-network is also described in Section III. Section IV proposes a new scheduling scheme for the corresponding vr-network. Section V combines the new vr-network and the scheduling scheme and prove that the combined solution achieves the optimal stability region of any possible INC schemes. In Sections II to V, we focus exclusively on time-varying channels. In Section V-A, we further generalize the proposed solution for rate adaptation and show numerically that it again achieves the optimal stability region.

Related Results: The most related works are [6], [9]–[11], which provide either a policy-based or a BP-based scheduling scheme for downlink networks. While they all achieve the 2-flow capacity of fixed channel quality, they are strictly suboptimal for time-varying PECs and for rate-adaptation. Other works [18], [19] study the benefits of external side information with fixed channel quality and no rate-adaptation.

II. Problem Formulation and Existing Results

A. Problem Formulation — The Broadcast Erasure Channel

We model the 1-base-station/2-client downlink traffic as a broadcast packet erasure channel (PEC). See Fig. 3 for illustration. The base station is sometimes called the source s. Consider the following slotted transmission system.

Dynamic Arrival: We assume that each incoming session-i packet takes a value from a finite field $\mathsf{GF}(\varrho)$. In the beginning of every time slot t, there are $A_1(t)$ session-1 packets and $A_2(t)$ session-2 packets arriving at the source s. We assume that $A_1(t)$ and $A_2(t)$ are i.i.d. integer-valued random variables with mean $(\mathsf{E}\{A_1(t)\}, \mathsf{E}\{A_2(t)\}) = (R_1, R_2)$ and bounded support. Recall that X_i and Y_j, $i, j \in \mathbb{N}$, denote the session-1 and session-2 packets, respectively.

Time-Varying Channel: We model the time-varying channel quality by a random process $\mathsf{cq}(t)$, which decides the reception probability of the *broadcast PEC*. In all our proofs, we assume $\mathsf{cq}(t)$ is i.i.d. As will be seen, our scheme can be directly applied to Markovian $\mathsf{cq}(t)$ as well. Simulation shows that it also achieves the optimal stability region for Markovian $\mathsf{cq}(t)$ [7] (albeit without any analytical proof). Due to space limits, the simulation results for Markovian $\mathsf{cq}(t)$ are omitted.

Let CQ denote the support of $\mathsf{cq}(t)$ and we assume $|\mathsf{CQ}|$ is finite. For any $c \in \mathsf{CQ}$, we use f_c to denote the steady state frequency of $\mathsf{cq}(t) = c$. We assume $f_c > 0$ for all $c \in \mathsf{CQ}$.

Broadcast Packet Erasure Channel: For each time slot t, source s can transmit one packet, $W(t) \in \mathsf{GF}(\varrho)$, which will be received by a random subset of destinations $\{d_1, d_2\}$, and let $W_{\text{rcvd},i}(t) \in \{W(t), *\}$ denote the received packet at destination d_i in time t. That is, $W_{\text{rcvd},i}(t) = W(t)$ means that the packet is received successfully and $W_{\text{rcvd},i}(t) = *$, the erasure symbol, means that the received packet is corrupted and discarded completely. Specifically, there are 4 possible *reception status* $\{\overline{d_1}\overline{d_2}, d_1\overline{d_2}, \overline{d_1}d_2, d_1d_2\}$, e.g., the reception status $\mathsf{rcpt} = d_1\overline{d_2}$ means that the packet is received by d_1 but not d_2. The reception status probabilities can be described by a vector $\vec{p} \triangleq (p_{\overline{d_1}\overline{d_2}}, p_{d_1\overline{d_2}}, p_{\overline{d_1}d_2}, p_{d_1d_2})$. For example, $\vec{p} = (0, 0.5, 0.5, 0)$ means that every time we transmit a packet, with 0.5 probability it will be received by d_1 only and with 0.5 probability it will be received by d_2 only. In contrast, if we have $\vec{p} = (0, 0, 0, 1)$, then it means that the packet is always received by d_1 and d_2 simultaneously. Since our model allows arbitrary joint probability vector $\vec{p}$, it captures the scenarios in which the erasure events of d_1 and d_2 are dependent, e.g., when the erasures at d_1 and d_2 are caused by a common (random) interference source.

Opportunistic INC: Since the reception probability is decided by the channel quality, we write $\vec{p}(\mathsf{cq}(t))$ as a function of $\mathsf{cq}(t)$ at time t. In the beginning of time t, we assume that s is aware of the channel quality $\mathsf{cq}(t)$ (and thus knows $\vec{p}(\mathsf{cq}(t))$) so that s can opportunistically decide how to encode the packet for time t. See Fig. 3. This is motivated by Cognitive Radio, for which s can sense the channel first before transmission.

ACKnowledgement: In the end of time t, d_1 and d_2 will report back to s whether they have received the transmitted packet or not (ACK/NACK). A useful notation regarding the ACK feedback is as follows. We use a 2-dimensional *channel status vector* $\mathbf{Z}(t)$ to represent the channel reception status:

$$\mathbf{Z}(t) = (Z_{d_1}(t), Z_{d_2}(t)) \in \{*, 1\}^2$$

where "$*$" and "1" represent erasure and successful reception, respectively. For example, when s transmits a packet $W(t) \in \mathsf{GF}(\varrho)$ in time t, the destination d_1 receives $W_{\text{rcvd},1}(t) = W(t)$ if $Z_{d_1}(t) = 1$, and receives $W_{\text{rcvd},1}(t) = *$ if $Z_{d_1}(t) = *$.

Buffers: There are two buffers at s which stores the incoming session-1 packets and session-2 packets, respectively. Let $\mathsf{Buffer}_i(t)$ denote the collection of all session-i packets currently stored in buffer i in the beginning of time t.

Encoding, Buffer Management, and Decoding: For simplicity, we use $[\cdot]_1^t$ to denote the collection from time 1 to t. For example, $[A_1, \mathbf{Z}]_1^t \triangleq \{A_1(\tau), \mathbf{Z}(\tau) : \forall \tau \in \{1, 2, ..., t\}\}$. At each time t, an opportunistic INC solution is defined by an *encoding function* and two *buffer pruning functions:*

Encoding: In the *beginning* of time t, the coded packet $W(t)$ sent by s is expressed by

$$W(t) = f_{\mathsf{ENC},t}(\mathsf{Buffer}_1(t), \mathsf{Buffer}_2(t), [\mathbf{Z}]_1^{t-1}). \quad (1)$$

That is, the coded packet is generated by the packets that are still in the two buffers and by the past reception status feedback from time 1 to $t-1$.

Buffer Management: In the *end* of time t, we prune the

buffers by the following equation: For $i = 1, 2$,

$$\begin{aligned}\mathsf{Buffer}_i(t+1) = \mathsf{Buffer}_i(t) \backslash f_{\mathsf{PRUNE},i,t}([A_1, A_2, \mathbf{Z}]_1^t) \\ \cup \{\text{New session-}i \text{ packets arrived in time } t\}. \quad (2)\end{aligned}$$

That is, the buffer pruning function $f_{\mathsf{PRUNE},i,t}([A_1, A_2, \mathbf{Z}]_1^t)$ will decide which packets to remove from $\mathsf{Buffer}_i(t)$ based on the arrival and the packet delivery patterns from time 1 to t, while new packets will also be stored in the buffer. $\mathsf{Buffer}_i(t+1)$ will later be used for encoding in time $t+1$.

The encoding and the buffer pruning functions need to satisfy the following **Decodability Condition:** For every time t, there exist two decoding functions such that

$$\begin{aligned}(X_1, ..., X_{\sum_{\tau=1}^t A_1(\tau)}) = f_{\mathsf{DEC},1,t}([W_{\text{rcvd},1}]_1^t, \mathsf{Buffer}_1(t+1)) \\ (Y_1, ..., Y_{\sum_{\tau=1}^t A_2(\tau)}) = f_{\mathsf{DEC},2,t}([W_{\text{rcvd},2}]_1^t, \mathsf{Buffer}_2(t+1)).\end{aligned} \quad (3)$$

The intuition of the above decodability requirement (3) is as follows. If the pruning function (2) is very aggressive, then the buffer size at source s is small but there is some risk that some desired messages X_i may be "removed from $\mathsf{Buffer}_1(t)$ prematurely." That is, once X_i is removed, it can no longer be decoded at d_1 even if we send all the content in the remaining $\mathsf{Buffer}_1(t+1)$ directly to d_1. To avoid this undesired consequence, (3) imposes that the pruning function has to be conservative in the sense that if in the end of time t we let d_i directly access $\mathsf{Buffer}_i(t+1)$ at the source s, then together with what d_i has already received $[W_{\text{rcvd},i}]_1^t$, d_i should be able to fully recover all the session-i packets up to time t.

Definition 1: A queue length $q(t)$ is *mean-rate stable* [20] (sometimes known as sublinearly stable) if

$$\lim_{t\to\infty} \frac{\mathsf{E}\{|q(t)|\}}{t} = 0. \quad (4)$$

Definition 2: An arrival rate vector (R_1, R_2) is *mean-rate stable* if there exists an NC scheme described by $f_{\mathsf{ENC},t}$, $f_{\mathsf{PRUNE},1,t}$ and $f_{\mathsf{PRUNE},2,t}$ (which have to satisfy (3)) such that the sizes of $\mathsf{Buffer}_1(t)$ and $\mathsf{Buffer}_2(t)$ are mean-rate stable. The NC stability region is the collection of all mean-rate stable vectors (R_1, R_2).

The above definition of mean-rate stability is a strict generalization of the traditional stability definition of uncoded transmissions. For example, suppose we decide to *not* using NC. Then we simply set the encoder $f_{\mathsf{ENC},t}$ to always return either "X_i for some i" or "Y_j for some j". And we prune X_i from $\mathsf{Buffer}_1(t)$ (resp. Y_j from $\mathsf{Buffer}_2(t)$) if X_i (resp. Y_j) was delivered successfully to d_1 (resp. d_2). The decodability condition (3) holds naturally for the above $f_{\mathsf{ENC},t}$, $f_{\mathsf{PRUNE},1,t}$ and $f_{\mathsf{PRUNE},2,t}$ and the buffers are basically the packet queues in the traditional non-coding schemes. Our new stability definition is thus equivalent to the traditional one once we restrict to non-coding solutions only.

On the other hand, when NC is allowed, the situation changes significantly. For example, an arbitrary NC scheme may send a coded packet that is a linear sum of three packets, say $[X_3 + X_5 + Y_4]$. Suppose the linear sum is received by d_1. The NC scheme then needs to carefully decide whether to remove X_3 or X_5 or both from $\mathsf{Buffer}_1(t)$ and/or whether to remove Y_4 from $\mathsf{Buffer}_2(t)$. This is the reason why we specify an NC scheme not only by the encoder $f_{\mathsf{ENC},t}$ but also by the buffer management policy $f_{\mathsf{PRUNE},1,t}$ and $f_{\mathsf{PRUNE},2,t}$. Since our stability definition allows for arbitrary $f_{\mathsf{ENC},t}$, $f_{\mathsf{PRUNE},k,t}$ and $f_{\mathsf{PRUNE},2,t}$, it thus represents the largest possible stability region that can be achieved by any NC solutions.

B. Shannon Capacity Region

Reference [15] focuses on the above setting but considers the infinite backlog block-code design. We summarize the Shannon capacity result in [15] as follows.

Proposition 1: [Propositions 1 and 3, [15]] For the block-code setting with infinite backlog, the closure of all achievable rate vectors (R_1, R_2) can be characterized by $|\mathsf{CQ}|+12$ linear inequalities that involve $18 \cdot |\mathsf{CQ}| + 7$ non-negative auxiliary variables. As a result, the Shannon capacity region (R_1, R_2) can be explicitly computed by solving the corresponding LP problem. Detailed description of the LP problem can be found in [15], [21].

Since the block-code setting is less stringent than the dynamic arrival setting in this work, the above Shannon capacity region serves as an outer bound for the mean-rate stability region in Definition 2. Our goal is to design a dynamic INC scheme, of which the stability region matches the Shannon capacity region.

III. The Proposed New INC Operations

In this section, we aim to solve Challenge 1 in Section I. We first discuss the limitations of the existing works on the INC block code design. We then describe a new set of binary INC operations that is capable of achieving the block code capacity. As discussed in Section I and Fig. 2, knowing the best set of INC operations alone is not enough to achieve the largest stability region. Our new virtual network scheduler design will be presented separately in Section IV.

A. The 5 INC operations are no longer optimal

In Section I, we have detailed 3 INC operations: Non-Coding-1, Non-Coding-2, and Classic-XOR. Two additional INC operations are introduced in [11]: Degenerate-XOR-1 and Degenerate-XOR-2 as illustrated in Fig. 1(b). Specifically, Degenerate-XOR-1 is designed to handle the degenerate case in which $Q^1_{\{2\}}$ is non empty but $Q^2_{\{1\}} = \emptyset$. Namely, there is at least one X_i packet overheard by d_2 but there is no Y_j packet overheard by d_1. Not having such Y_j implies that one cannot send $[X_i + Y_j]$ (the Classic-XOR operation). An alternative is thus to send the overheard X_i uncodedly (as if sending $[X_i + 0]$). We term this operation Degenerate-XOR-1. One can see from Fig. 1(b) that Degenerate-XOR-1 takes a vr-packet from $Q^1_{\{2\}}$ as input. If d_1 receives it, the vr-packet will leave the vr-network. Degenerate-XOR-2 is the symmetric version of Degenerate-XOR-1.

We use the following example to illustrate the sub-optimality of the above 5 operations. Suppose s has an X packet for d_1 and a Y packet for d_2 and consider a duration

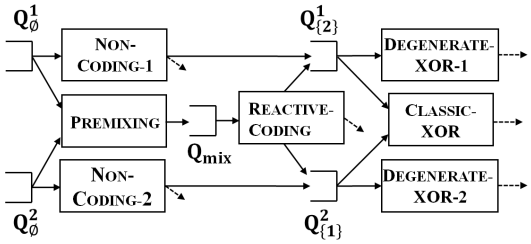

Fig. 4. The virtual network of the proposed new INC solution.

of 2 time slots. Also suppose that s knows beforehand that the time-varying channel will have (i) $\vec{p} = (0, 0.5, 0.5, 0)$ for slot 1; and (ii) $\vec{p} = (0, 0, 0, 1)$ for slot 2. The goal is to transmit as many packets in 2 time slots as possible.

Solution 1: INC based on the 5 operations in Fig. 1(b). In the beginning of time 1, both $Q^1_{\{2\}}$ and $Q^2_{\{1\}}$ are empty. Therefore, we can only choose either NON-CODING-1 or NON-CODING-2. Without loss of generality we choose NON-CODING-1 and send X uncodedly. Since $\vec{p} = (0, 0.5, 0.5, 0)$ in slot 1, there are only two cases to consider. Case 1: X is received only by d_1. In this case, we can send Y in the second time slot, which is guaranteed to arrive at d_2 since $\vec{p} = (0, 0, 0, 1)$ in slot 2. The total sum rate is sending 2 packets (X and Y) in 2 time slots. Case 2: X is received only by d_2. In this case, $Q^1_{\{2\}}$ contains one packet X, and $Q^2_\emptyset$ contains one packet Y, and all the other queues in Fig. 1(b) are empty. We can thus choose either NON-CODING-2 or DEGENERATE-XOR-1 for slot 2. Regardless of which coding operation we choose, slot 2 will then deliver 1 packet to either d_2 or d_1, depending on the INC operation we choose. Since no packet is delivered in slot 1, the total sum rate is 1 packet in 2 time slots. Since both cases have probability 0.5, the expected sum rate is $2 \cdot 0.5 + 1 \cdot 0.5 = 1.5$ packets in 2 time slots.

An optimal solution: We can achieve strictly better throughput by introducing new INC operations. Specifically, in slot 1, we send the linear sum $[X + Y]$ *even though neither X nor Y has ever been transmitted*, a distinct departure from the existing 5-operation-based solutions.

Again consider two cases: Case 1: $[X+Y]$ is received only by d_1. In this case, we let s send Y uncodedly in slot 2. Since $\vec{p} = (0, 0, 0, 1)$ in slot 2, Y will be received by both d_1 and d_2. d_2 is happy since it has now received the desired Y packet. d_1 can use Y together with the $[X + Y]$ packet received in slot 1 to decode its desired X packet. Therefore, we deliver 2 packets (X and Y) in 2 time slots. Case 2: $[X+Y]$ is received only by d_2. In this case, we let s send X uncodedly in slot 2. By the symmetric arguments, we deliver 2 packets (X and Y) in 2 time slots. The sum-rate of the new solution is 2 packets in 2 slots, a 33% improvement over the existing solution.

Remark: This example focuses on a 2-time-slot duration due to the simplicity of the analysis. It is worth noting that the throughput improvement persists even for infinitely many time slots. See the simulation results in Section VI.

The above example shows that the set of 5 INC operations: NON-CODING-1, NON-CODING-2, CLASSIC-XOR, DEGENERATE-XOR-1, and DEGENERATE-XOR-2 is not capable of achieving the Shannon capacity. To mitigate this inefficiency, we will enlarge the above set by introducing two more INC operations. We will first describe the corresponding encoder and then discuss the decoder and buffer management.

B. Encoding Steps

We start from Fig. 1(b), the vr-network corresponding to the existing 5 INC operations. We then add 2 more operations, termed PREMIXING and REACTIVE-CODING, respectively, and 1 new virtual queue, termed Q_{mix}, and plot the vr-network of the new scheme in Fig. 4. From Fig. 4, we can clearly see that PREMIXING involves both $Q^1_\emptyset$ and $Q^2_\emptyset$ as input and outputs to Q_{mix}. REACTIVE-CODING involves Q_{mix} as input and outputs to $Q^1_{\{2\}}$ or $Q^2_{\{1\}}$ or simply lets the vr-packet leave the vr-network (described by the dotted arrow).

In the following, we describe in detail how these two new INC operations work and how to integrate them with the other 5 operations. Our description contains 4 parts.

Part I: The two operations, NON-CODING-1 and NON-CODING-2, remain the same. That is, if we choose NON-CODING-1, then s chooses an uncoded session-1 packet X_i from $Q^1_\emptyset$ and send it out. NON-CODING-2 is symmetric.

Part II: We now describe the new operation PREMIXING. We can choose PREMIXING only if both $Q^1_\emptyset$ and $Q^2_\emptyset$ are non-empty. Namely, there are $\{X_i\}$ packets and $\{Y_j\}$ packets that have not been heard by any of d_1 and d_2. Whenever we schedule PREMIXING, we choose one X_i from $Q^1_\emptyset$ and one Y_j from $Q^2_\emptyset$ and send $[X_i + Y_j]$. If neither d_1 nor d_2 receives it, both X_i and Y_j remain in their original queues.

If at least one of $\{d_1, d_2\}$ receives it, we remove *both* X_i and Y_j from their queues and insert a tuple $(\mathsf{rcpt}; X_i, Y_j)$ into Q_{mix}. That is, unlike the other queues for which each entry is a single vr-packet, each entry of Q_{mix} is a tuple.

The first coordinate of $(\mathsf{rcpt}; X_i, Y_j)$ is rcpt, the reception status of $[X_i + Y_j]$. For example, if $[X_i + Y_j]$ was received by d_2 but not by d_1, then we set/record $\mathsf{rcpt} = \overline{d_1} d_2$; If $[X_i + Y_j]$ was received by both d_1 and d_2, then $\mathsf{rcpt} = d_1 d_2$. The second and third coordinates store the participating packets X_i and Y_j separately. The reason why we do not store the linear sum directly is due to the new REACTIVE-CODING operation.

Part III: We now describe the new operation REACTIVE-CODING. For any time t, we can choose REACTIVE-CODING only if there is at least one tuple $(\mathsf{rcpt}; X_i, Y_j)$ in Q_{mix}. Choose one tuple from Q_{mix} and denote it by $(\mathsf{rcpt}^*; X_i^*, Y_j^*)$. We now describe the encoding part of REACTIVE-CODING.

If $\mathsf{rcpt}^* = d_1 \overline{d_2}$, we send Y_j^*. If $\mathsf{rcpt}^* = \overline{d_1} d_2$ or $d_1 d_2$, we send X_i^*. One can see that the coding operation depends on the reception status rcpt^* when $[X_i^* + Y_j^*]$ was first transmitted. This is why it is named REACTIVE-CODING.

The movement of the vr-packets depends on the current reception status of time t, denoted by $\mathsf{rcpt}(t)$, and also on the old reception status rcpt^* when the sum $[X_i^* + Y_j^*]$ was originally transmitted. The detailed movement rules are described in Table I. The way to interpret the table is as follows. When $\mathsf{rcpt}(t) = \overline{d_1 d_2}$, i.e., neither d_1 nor d_2 receives the current transmission, then we do nothing, i.e., keep the tuple inside Q_{mix}. On the other hand, we remove the tuple from Q_{mix} whenever $\mathsf{rcpt}(t) \in \{d_1 \overline{d_2}, \overline{d_1} d_2, d_1 d_2\}$. If $\mathsf{rcpt}(t) = d_1 d_2$,

TABLE I
A SUMMARY OF THE REACTIVE-CODING OPERATION

Current Reception Status $\mathbf{rcpt}(t)$	Departure	Insertion		
		$\mathbf{rcpt}^*=d_1\overline{d_2}$ (Send Y_j^*)	$\mathbf{rcpt}^*=\overline{d_1}d_2$ (Send X_i^*)	$\mathbf{rcpt}^*=d_1d_2$ (Send X_i^*)
$d_1\overline{d_2}$	Remove the tuple from Q_{mix}	Insert Y_j^* to $Q^2_{\{1\}}$	Insert X_i^* to $Q^2_{\{1\}}$	Insert Y_j^* to $Q^2_{\{1\}}$
$\overline{d_1}d_2$		Insert Y_j^* to $Q^1_{\{2\}}$	Insert X_i^* to $Q^1_{\{2\}}$	Insert X_i^* to $Q^1_{\{2\}}$
d_1d_2		Do not insert any packet back into the virtual network.		
$\overline{d_1d_2}$	Do nothing			

TABLE II
A SUMMARY OF THE TRANSITION PROBABILITY OF THE VIRTUAL NETWORK IN FIG. 4, WHERE $p_{d_1\vee d_2} \triangleq p_{d_1\overline{d_2}} + p_{\overline{d_1}d_2} + p_{d_1d_2}$; $p_{d_1} \triangleq p_{d_1\overline{d_2}} + p_{d_1d_2}$; NC1 STANDS FOR NON-CODING-1; CX STANDS FOR CLASSIC-XOR; DX1 STANDS FOR DEGENERATE-XOR-1; PM STANDS FOR PREMIXING; RC STANDS FOR REACTIVE-CODING.

Edge	Trans. Prob.	Edge	Trans. Prob.
$Q^1_\emptyset \to$NC1	$p_{d_1\vee d_2}$	$Q^1_\emptyset \to$PM	$p_{d_1\vee d_2}$
NC1$\to Q^1_{\{2\}}$	$p_{\overline{d_1}d_2}$	PM$\to Q_{\text{mix}}$	$p_{d_1\vee d_2}$
$Q^1_{\{2\}} \to$DX1	p_{d_1}	$Q_{\text{mix}} \to$RC	$p_{d_1\vee d_2}$
$Q^1_{\{2\}} \to$CX	p_{d_1}	RC$\to Q^1_{\{2\}}$	$p_{\overline{d_1}d_2}$

then we remove the tuple but do not insert any vr-packet back to the vr-network, see the second last row of Table I. The tuple essentially leaves the vr-network in this case. If $\mathsf{rcpt}(t) = d_1\overline{d_2}$ and $\mathsf{rcpt}^* = d_1d_2$, then we remove the tuple from Q_{mix} and insert Y_j^* to $Q^2_{\{1\}}$. The rest of the combinations can be read from Table I in the same way. One can verify that the optimal INC example introduced in Section III-A is a direct application of the PREMIXING and REACTIVE-CODING operations.

Before proceeding, we briefly explain why the combination of PREMIXING and REACTIVE-CODING works. To facilitate discussion, we call the time slot in which we use PREMIXING to transmit $[X_i^* + Y_j^*]$ "slot 1" and the time slot in which we use REACTIVE-CODING "slot 2," even though the coding operations PREMIXING and REACTIVE-CODING may not be scheduled in two adjacent time slots. Using this notation, if $\mathsf{rcpt}^* = d_1\overline{d_2}$ and $\mathsf{rcpt}(t) = d_1d_2$, then it means that d_1 receives $[X_i^* + Y_j^*]$ and Y_j^* in slots 1 and 2, respectively and d_2 receives Y_j^* in slot 2. In this case, d_1 can decode the desired X_i^* and d_2 directly receives the desired Y_j^*. We now consider the perspective of the vr-network. Table I shows that the tuple will be removed from Q_{mix} and leave the vr-network. Therefore, no queue in the vr-network stores any of X_i^* and Y_j^*. This correctly reflects the fact that both X_i^* and Y_j^* have been received by their intended destinations.

Another example is when $\mathsf{rcpt}^* = \overline{d_1}d_2$ and $\mathsf{rcpt}(t) = d_1\overline{d_2}$. In this case, d_2 receives $[X_i^* + Y_j^*]$ in slot 1 and d_1 receives X_i^* in slot 2. From the vr-network's perspective, the movement rule (see Table I) removes the tuple from Q_{mix} and insert an X_i^* packet to $Q^2_{\{1\}}$. Since a vr-packet is removed from a session-1 queue[3] Q_{mix} and inserted to a session-2 queue $Q^2_{\{1\}}$, the total number of vr-packets in the session-1 queue decreases by 1. This correctly reflects the fact that d_1 has received 1 desired packet X_i^* in slot 2.

An astute reader may wonder why in this example we can put X_i^*, a session-1 packet, into a session-2 queue $Q^2_{\{1\}}$. The reason is that whenever d_2 receives X_i^* in the future, it can recover its desired Y_j^* by subtracting X_i^* from the linear sum $[X_i^* + Y_j^*]$ it received in slot 1 (recall that $\mathsf{rcpt}^* = d_1\overline{d_2}$.) Therefore, X_i^* is now information-equivalent to Y_j^*, a session-2 packet. Moreover, d_1 has received X_i^*. Therefore, in terms of the information it carries, X_i^* is no different than a session-2 packet that has been overheard by d_1. As a result, it is fit to put X_i^* in $Q^2_{\{1\}}$.

Part IV: We now describe some slight modification to CLASSIC-XOR, DEGENERATE-XOR-1, and DEGENERATE-XOR-2. A unique feature of the new scheme is that some packets in $Q^2_{\{1\}}$ may be an X_i^* packet that is inserted by REACTIVE-CODING when $\mathsf{rcpt}^* = \overline{d_1}d_2$ and $\mathsf{rcpt}(t) = d_1\overline{d_2}$. (Also some $Q^1_{\{2\}}$ packets may be Y_j^*.) However, in our previous discussion, we have shown such an X_i^* in $Q^2_{\{1\}}$ is information-equivalent to a Y_j^* packet overheard by d_1. Therefore, in the CLASSIC-XOR operation, we should not insist on sending $[X_i + Y_j]$ but can also send $[P_1 + P_2]$ as long as P_1 is from $Q^1_{\{2\}}$ and P_2 is from $Q^2_{\{1\}}$. The same relaxation must be applied to DEGENERATE-XOR-1 and DEGENERATE-XOR-2 operations. Other than this slight relaxation, the three operations work in the same way as previously described in Sections I and III-A.

We conclude this section by listing in Table II the transition probabilities of half of the edges of the vr-network in Fig. 4. E.g., when we schedule PREMIXING, we remove a packet from $Q^1_\emptyset$ if at least one of $\{d_1, d_2\}$ receives it. The transition probability along the $Q^1_\emptyset \to$PREMIXING edge is thus $p_{d_1\vee d_2} \triangleq p_{d_1\overline{d_2}} + p_{\overline{d_1}d_2} + p_{d_1d_2}$. All the other transition probabilities in Table II can be derived similarly. The transition probability of the rest of the edges can be derived by symmetry.

C. Decoding and Buffer Management at Receivers

The vr-network is a conceptual tool used by s to decide what to transmit in each time slot. As a result, for encoding, s only needs to store in its memory all the packets that are currently in the vr-network. This implies that as long as the queues in the vr-network are stable, the actual memory usage (buffer size) at the source is also stable. However, one also needs to ensure that the memory usage for receivers is stable as well. In this subsection we discuss the decoding operations and the memory usage at the receivers.

A very commonly used assumption in the Shannon-capacity literature is to assume that the receivers store all the overheard packets so that they can use them to decode any XORed packets sent from the source. No packets will ever be removed from the buffer under such a policy. Obviously, such an infinite-buffer scheme is highly impractical.

When there is only 1 session in the network, Gaussian elimination (GE) is often used for buffer management. However, generalizing GE for the multi-session non-generation-based schemes can be very complicated [22].

[3] Q_{mix} is regarded as both a session-1 and a session-2 queue simultaneously.

In the existing multi-session INC works [5], [6], [9], [10], a commonly used buffer management scheme is the following. For any time t, define i^* (resp. j^*) as the smallest i (resp. j) such that d_1 (resp. d_2) has not decoded X_i (resp. Y_j) in the end of time t. Then each receiver can simply remove any X_i and Y_j from its buffer for those $i < i^*$ and $j < j^*$. The reason is that since those X_i and Y_j have already been known by their intended receivers, they will not participate in any future transmission, and thus can be removed from the buffer.

On the other hand, under such a buffer management scheme, the receivers may use significantly more memory than that of the source. The reason is as follows. Suppose d_1 has decoded X_1, X_3, $X_4, \cdots, X_8$, and X_{10} and suppose d_2 has decoded Y_1 to Y_4 and Y_6 to Y_{10}. In this case $i^* = 2$ and $j^* = 5$. The aforementioned scheme will keep all X_2 to X_{10} in the buffer of d_2 and all Y_5 to Y_{10} in the buffer of d_1 even though the source is interested in only sending 3 more packets X_2, X_9, and Y_5. The above buffer management scheme is too conservative since it does not trace the actual overhearing status of each packet and only use i^* and j^* to decide whether to prune the packets in the buffers of the receivers.

In contrast, our vr-network scheme admits the following efficient decoding operations and buffer management. In the following, we describe the decoding and buffer management at d_1. The operations at d_2 can be done symmetrically. Our description consists of two parts. We first describe how to perform decoding at d_1 and which packets need to be stored in d_1's buffer, *while assuming that any packets that have ever been stored in the buffer will never be expunged.* In the second part, we describe how to prune the memory usage without affecting the decoding operations.

Upon d_1 receiving a packet: Case 1: If the received packet is generated by NON-CODING-1, then such a packet must be X_i for some i. We thus pass such an X_i to the upper layer; Case 2: If the received packet is generated by NON-CODING-2, then such a packet must be Y_j for some j. We store Y_j in the buffer of d_1; Case 3: If the received packet is generated by PREMIXING, then such a packet must be $[X_i + Y_j]$. We store the linear sum $[X_i + Y_j]$ in the buffer. Case 4: If the received packet is generated by REACTIVE CODING , then such a packet can be either X_i^* or Y_j^*, see Table I.

We have two sub-cases in this scenario. Case 4.1: If the packet is X_i^*, we pass such an X_i^* to the upper layer. Then d_1 examines whether it has stored $[X_i^* + Y_j^*]$ in its buffer. If so, use X_i^* to decode Y_j^* and insert Y_j^* to the buffer. If not, store a separate copy of X_i^* in the buffer even though one copy of X_i^* has already been passed to the upper layer. Case 4.2: If the packet is Y_j^*, then by Table I d_1 must have received the linear sum $[X_i^* + Y_j^*]$ in the corresponding PREMIXING operation in the past. Therefore, $[X_i^* + Y_j^*]$ must be in the buffer of d_1 already. We can thus use Y_j^* and $[X_i^* + Y_j^*]$ to decode the desired X_i^*. Receiver d_1 then passes the decoded X_i^* to the upper layer and stores Y_j^* in its buffer.

Case 5: If the received packet is generated by DEGENERATE XOR-1, then such a packet can be either X_i or Y_j, where Y_j are those packets in $Q^1_{\{2\}}$ but coming from REACTIVE CODING, see Fig. 4. Case 5.1: If the packet is X_i, we pass such an X_i to the upper layer. Case 5.2: If the packet is Y_j, then from Table I, it must be corresponding to the intersection of the row of $\mathsf{rcpt} = \overline{d_1} d_2$ and the column of $\mathsf{rcpt}^* = d_1 \overline{d_2}$. As a result, d_1 must have received the corresponding $[X_i + Y_j]$ in the PREMIXING operation. d_1 can thus use the received Y_j to decode the desired X_i and then pass X_i to the upper layer.

Case 6: the received packet is generated by DEGENERATE XOR-2. Consider two subcases. Case 6.1: the received packet is X_i. It is clear from Fig. 4 that such X_i must come from REACTIVE-CODING since any packet from $Q^2_\emptyset$ to $Q^2_{\{1\}}$ must be a Y_j packet. By Table I and the row corresponding to $\mathsf{rcpt} = d_1 \overline{d_2}$, any $X_i \in Q^2_{\{1\}}$ that came from REACTIVE-CODING must correspond to the column of $\mathsf{rcpt}^* = \overline{d_1} d_2$. By the second half of Case 4.1, such $X_i \in Q^2_{\{1\}}$ must be in the buffer of d_1 already. As a result, d_1 can simply ignore any X_i packet it receives from DEGENERATE XOR-2. Case 6.2: the received packet is Y_j. By the discussion of Case 2, if the $Y_j \in Q^2_{\{1\}}$ came from NON-CODING-2, then it must be in the buffer of d_1 already. As a result, d_1 can simply ignore those Y_j packets. If the $Y_j \in Q^2_{\{1\}}$ came from REACTIVE-CODING, then by Table I and the row corresponding to $\mathsf{rcpt} = d_1 \overline{d_2}$, those $Y_j \in Q^2_{\{1\}}$ must correspond to the column of either $\mathsf{rcpt}^* = d_1 \overline{d_2}$ or $\mathsf{rcpt}^* = d_1 d_2$. By the first half of Case 4.1 and by Case 4.2, such $Y_j \in Q^2_{\{1\}}$ must be in the buffer of d_1 already. Again, d_1 can simply ignore those Y_j packets. From the discussion of Cases 6.1 and 6.2, *any packet generated by* DEGENERATE XOR-2 *is already known to d_1, and nothing needs to be done in this case.*[4]

Case 7: the received packet is generated by CLASSIC-XOR. Since we have shown in Case 6 that any packet in $Q^2_{\{1\}}$ is known to d_1, receiver d_1 can simply subtract the $Q^2_{\{1\}}$ packet from the linear sum received in Case 7. As a result, from d_1's perspective, it is no different than directly receiving a $Q^1_{\{2\}}$ packet, i.e., Case 5. d_1 thus repeats the decoding operation and buffer management in the same way as in Case 5.

Periodically pruning the memory: In the above discussion, we elaborate which packets d_1 should store in its buffer and how to use them for decoding, while assuming no packet will ever be removed from the buffer. In the following, we discuss how to remove packets from the buffer of d_1.

We first notice that by the discussion of Cases 1 to 7, the uncoded packets in the buffer of d_1, i.e., those of the form of either X_i or Y_j, are used for decoding *only in the scenario of Case 7*. Namely, they are used to remove the $Q^2_{\{1\}}$ packet participating in the linear sum of CLASSIC-XOR. As a result, periodically we let s send to d_1 the list of all packets in $Q^2_{\{1\}}$. After receiving the list, d_1 simply removes from its buffer any uncoded packets X_i and/or Y_j that are no longer in $Q^2_{\{1\}}$.

We then notice that by the discussion of Cases 1 to 7, the linear sum $[X_i + Y_j]$ in the buffer of d_1 is only used in one of the following two scenarios: (i) To decode Y_j in Case 4.1 or to decode X_i in Case 4.2; and (ii) To decode X_i in Case 5.2. As a result, the $[X_i + Y_j]$ in the buffer is "useful" only if one of the following two conditions are satisfied: (a) The corresponding tuple $(\mathsf{rcpt}, X_i, Y_j)$ is still in Q_{mix}, which corresponds to the

[4]Cases 5 and 6 echoes our previous arguments that any packet in $Q^2_{\{1\}}$ (which can be either X_i or Y_j) is information-equivalent to a session-2 packet that has been overheard by d_1.

scenarios of Cases 4.1 and 4.2; and (b) If the participating Y_j is still in $Q^1_{\{2\}}$. By the above observation, periodically we let s send to d_1 the list of all packets in $Q^1_{\{2\}}$ and Q_{mix}. After receiving the list, d_1 simply removes from its buffer any linear sum $[X_i + Y_j]$ that satisfies neither (a) nor (b).

The above pruning mechanism ensures that only the packets useful for future decoding are kept in the buffer of d_1 and d_2. Furthermore, it also leads to the following lemma.

Lemma 1: Assume the lists of packets in $Q^1_{\{2\}}$, $Q^2_{\{1\}}$, and Q_{mix} are sent to d_1 after every time slot. The number of packets in the buffer of d_1 is upper bounded by $|Q^1_{\{2\}}|+|Q^2_{\{1\}}|+|Q_{\text{mix}}|$.

The proof of Lemma 1 is provided in [21].

Lemma 1 implies that as long as the queues in the vr-network are stabilized, the actual memory usage at both the source and the destinations can be stabilized simultaneously.

Remark: Each transmitted packet is either an uncoded packet or a binary-XOR of two packets. Therefore, during transmission we only need to store 1 or 2 packet sequence numbers in the header of the uncoded/coded packet, depending on whether we send an uncoded packet or a linear sum. The overhead of updating the packet list is omitted but we can choose only to update it periodically. The communication overhead of the proposed scheme is thus small.

IV. The Proposed Scheduling Solution

In this section, we aim to solve Challenge 2 in Section I. The main tool that we use to stabilize the vr-network is stochastic processing networks (SPNs). In the following, we will discuss the basic definitions, existing results on a special class of SPNs, and our throughput-optimal scheduling solution.

A. The Main Features of SPNs

The SPN is a generalization of the store-and-forward networks. In an SPN, a packet cannot be transmitted directly from one queue to another queue through links. Instead, it must first be processed by a unit called "Service Activity" (SA). The SA first collects a certain amount of packets from one or more queues (named the *input queues*), jointly processes/consumes these packets, generates a new set of packets, and finally redistributes them to another set of queues (named the *output queues*). The number of consumed packets may be different than the number of generated packets. There is one critical rule: *An SA can be activated only when all its input queues can provide enough amount of packets for the SA to process.* This rule captures directly the INC behavior and thus makes INC a natural application of SPNs. Other applications of SPNs include the video streaming and Map-&-Reduce scheduling.

All the existing SPN scheduling solutions [16], [17] assume a special class of SPNs, which we call SPNs with deterministic departure, which is quite different from our INC-based vr-network. The reason is as follows. When a packet is broadcast by s, it can arrive at a random subset of receivers. Therefore, the vr-packets move among the vr-queues according to some probability distribution. We call the SPN model that allows random departure service rates "the SPN with random departure." It turns out that random departure presents a unique challenge for SPN scheduling. See [16] for an example of such a challenge and also see the discussion in [21].

B. A Simple SPN Model with Random Departure

We now formally define a random SPN model that includes the INC vr-network in Section III as a special example. Consider a time-slotted system with i.i.d. channel quality $\mathsf{cq}(t)$. A (0,1) random SPN consists of three components: the input activities (IAs), the service activities (SAs), and the queues. Suppose that there are K queues, M IAs, and N SAs.

Input Activities: Each IA represents a session (or a flow) of packets. Specifically, when an IA m is activated, it injects a deterministic number of $\alpha_{k,m}$ packets to queue k where $\alpha_{k,m}$ is of integer value. We use $\mathcal{A} \in \mathbb{R}^{K\times M}$ to denote the "input matrix" with the (k,m)-th entry equals to $\alpha_{k,m}$, for all m and k. At each time t, a random subset of IAs will be activated. Equivalently, we define $\mathbf{a}(t) \triangleq (a_1(t), a_2(t), \cdots, a_M(t)) \in \{0,1\}^M$ as the random "arrival vector" at time t. If $a_m(t) = 1$, then IA m is activated at time t. We assume that the random vector $\mathbf{a}(t)$ is i.i.d. over time with the average rate vector $\mathbf{R} = \mathsf{E}\{\mathbf{a}(t)\}$. In our setting, the $\mathcal{A}$ matrix is a fixed (deterministic) system parameter and all the randomness of IAs lies in $\mathbf{a}(t)$.

Service Activities: For each service activity SA n, we define the *input queues* of SA n as the queues which are required to provide some packets when SA n is activated. Let $\mathcal{I}_n$ denote the collection of the input queues of SA n. Similarly, we define the *output queues* of SA n as the queues which will possibly receive packets when SA n is activated, and let $\mathcal{O}_n$ be the collection of the output queues of SA n. I.e., when SA n is activated, it consumes packets from queues in $\mathcal{I}_n$, and generates new packets and sends them to queues in $\mathcal{O}_n$. We assume that $\mathsf{cq}(t)$ does not change $\mathcal{I}_n$ and $\mathcal{O}_n$.

There are 3 SA-activation rules in a (0,1) random SPN:

SA-Activation Rule 1: SA n can be activated only if for all $k \in \mathcal{I}_n$, queue k has at least 1 packet in the queue. For future reference, we say SA n is *feasible* at time t if at time t queue k has at least 1 packet for all $k \in \mathcal{I}_n$. Otherwise, we say SA n is infeasible at time t.

SA-Activation Rule 2: When SA n is activated with the channel quality c (assuming SA n is feasible), the number of packets leaving queue k is a binary random variable, $\beta^{\text{in}}_{k,n}(c)$, with mean $\overline{\beta^{\text{in}}_{k,n}(c)}$ for all $k \in \mathcal{I}_n$.

Note that there is a subtlety in Rules 1 and 2. By Rule 2, when we activate an SA n, it sometimes consumes zero packet from its input queues. However, even if it may consume zero packet, Rule 1 imposes that all input queues must always have at least 1 packet before we can activate an SA. Such a subtlety is important for our vr-network. For example, we can schedule PREMIXING in Fig. 4 only when both $Q^1_\emptyset$ and $Q^2_\emptyset$ are non-empty. But whether PREMIXING actually consumes any $Q^1_\emptyset$ and $Q^2_\emptyset$ packets depending on the random reception event of the transmission.

SA-Activation Rule 3: When SA n is activated with the channel quality c (assuming SA n is feasible), the number of packets entering queue k is a binary random variable, $\beta^{\text{out}}_{k,n}(c)$, with mean $\overline{\beta^{\text{out}}_{k,n}(c)}$ for all $k \in \mathcal{O}_n$.

Let $\mathcal{B}^{\text{in}}(c) \in \mathbb{R}^{K*N}$ be the *random input service matrix* under channel quality c with the (k,n)-entry equals to $\beta^{\text{in}}_{k,n}(c)$, and let $\mathcal{B}^{\text{out}}(c) \in \mathbb{R}^{K*N}$ be the *random output service matrix* under channel quality c with the (k,n)-entry equals to $\beta^{\text{out}}_{k,n}(c)$.

The expectations of $\mathcal{B}^{\text{in}}(c)$ and $\mathcal{B}^{\text{out}}(c)$ are denoted by $\overline{\mathcal{B}^{\text{in}}(c)}$ and $\overline{\mathcal{B}^{\text{out}}(c)}$, respectively. We assume that given any channel quality $c \in \mathsf{CQ}$, both the input and output service matrix $\mathcal{B}^{\text{in}}(c)$ and $\mathcal{B}^{\text{out}}(c)$ are independently distributed over time.

Scheduling of the SAs: At the beginning of each time t, the SPN scheduler is made aware of the current channel quality $\mathsf{cq}(t)$ and can choose to "activate" at most one SA. Let $\mathbf{x}(t) \in \{0,1\}^N$ be the "service vector" at time t. If the n-th coordinate $\mathbf{x}_n(t) = 1$, then it implies that we choose to activate SA n at time t. Let $\mathfrak{X}$ denote the set of vectors that contains all Dirac delta vectors and the all-zero vector, i.e., those vectors that can be activated at any given time slot. Define Λ to be the convex hull of $\mathfrak{X}$ and let Λ° be the interior of Λ.

Other Technical Assumptions: We also use the following 2 technical assumptions. Assumption 1: The input/output queues $\mathcal{I}_n$ and $\mathcal{O}_n$ of the SAs can be used to plot the corresponding SPN. We assume that the corresponding SPN is acyclic. Assumption 2: For any $\mathsf{cq}(t) = c$, the expectation of $\beta^{\text{in}}_{k,n}(c)$ (resp. $\beta^{\text{out}}_{k,n}(c)$) with $k \in \mathcal{I}_n$ (resp. $k \in \mathcal{O}_n$) is in $(0,1]$. Assumptions 1 and 2 are used to rigorously prove the mean-rate stability region, which eliminate, respectively, the cyclic setting and the limiting case in which the Bernoulli random variables are always 0.

One can easily verify that the above (0,1) random SPN model includes the vr-network in Fig. 4 as a special example.

C. The Proposed Scheduler For (0,1) Random SPNs

We borrow the wisdom of deficit maximum weight (DMW) scheduling [16]. Specifically, our scheduler maintains a real-valued counter $q_k(t)$, called the virtual queue length, for each queue k. Initially, $q_k(1)$ is set to 0. For comparison, the actual queue length is denoted by $Q_k(t)$.

The key feature of the scheduler is that it makes its decision based on $q_k(t)$ instead of $Q_k(t)$. Specifically, for each time t, we compute the "preferred[5] service vector" by

$$\mathbf{x}^*(t) = \arg\max_{\mathbf{x}\in\mathfrak{X}} \mathbf{d}^{\mathsf{T}}(t)\cdot\mathbf{x}, \tag{5}$$

$$\text{where} \qquad \mathbf{d}(t) = \left(\overline{\mathcal{B}^{\text{in}}(\mathsf{cq}(t))} - \overline{\mathcal{B}^{\text{out}}(\mathsf{cq}(t))}\right)^{\mathsf{T}} \mathbf{q}(t) \tag{6}$$

is the back pressure vector; $\mathbf{q}(t)$ is the vector of the virtual queue lengths; and we recall that the notations $\overline{\mathcal{B}^{\text{in}}(\mathsf{cq}(t))}$ and $\overline{\mathcal{B}^{\text{out}}(\mathsf{cq}(t))}$ are the expectations when the channel quality $\mathsf{cq}(t) = c$. Since we assume that each vector in $\mathfrak{X}$ has at most 1 non-zero coordinate, (5) and (6) basically find the preferred SA n^* in time t. We then check whether the preferred SA n^* is feasible. If so, we officially schedule SA n^*. If not, we let the system to be idle,[6] i.e., the actually scheduled service vector $\mathbf{x}(t) = \mathbf{0}$ is now all-zero.

Regardless of whether the preferred SA n^* is feasible or not, we update $\mathbf{q}(t)$ by:

$$\begin{aligned}\mathbf{q}(t+1) =& \mathbf{q}(t) + \mathcal{A}\cdot\mathbf{a}(t)\\ &+ \left(\overline{\mathcal{B}^{\text{out}}(\mathsf{cq}(t))} - \overline{\mathcal{B}^{\text{in}}(\mathsf{cq}(t))}\right)\cdot\mathbf{x}^*(t).\end{aligned} \tag{7}$$

Note that the actual queue length $Q_k(t)$ is updated in a way very different from (7). If the preferred SA n^* is not feasible, then the system remains idle and $Q_k(t)$ changes if and only if there is any new packet arrival. If SA n^* is feasible, then $Q_k(t)$ is updated based on the actual packet movement. While the actual queue lengths $Q_k(t)$ is always ≥ 0, the virtual queue length $\mathbf{q}(t)$ can be strictly negative when updated via (7).

The above scheduling scheme is denoted by $\mathsf{SCH}_{\text{avg}}$ since (7) is based on the average departure rate.

D. Performance Analysis

The following two propositions characterize the mean-rate stability region of any (0,1) random SPN.

Proposition 2: A rate vector $\mathbf{R}$ can be mean-rate stabilized only if there exist $\mathbf{s}_c \in \Lambda$ for all $c \in \mathsf{CQ}$ such that

$$\mathcal{A}\cdot\mathbf{R} + \sum_{c\in\mathsf{CQ}} f_c \cdot \overline{\mathcal{B}^{\text{out}}(c)}\cdot\mathbf{s}_c = \sum_{c\in\mathsf{CQ}} f_c\cdot\overline{\mathcal{B}^{\text{in}}(c)}\cdot\mathbf{s}_c. \tag{8}$$

Proposition 2 can be derived by conventional flow conservation arguments as in [16] and the proof is thus omitted.

Proposition 3: For any rate vector $\mathbf{R}$, if there exist $\mathbf{s}_c \in \Lambda^\circ$ for all $c \in \mathsf{CQ}$ such that (8) holds, then the proposed scheme $\mathsf{SCH}_{\text{avg}}$ in Section IV-C can mean-rate stabilize the (0,1) random SPN with arrival rate $\mathbf{R}$.

Outline of the proof of Proposition 3: Let each queue k keep another two real-valued counters $q^{\text{inter}}_k(t)$ and $Q^{\text{inter}}_k(t)$, termed the *intermediate virtual queue length* and *intermediate actual queue length*. There are thus 4 different queue length values[7] $q_k(t)$, $q^{\text{inter}}_k(t)$, $Q^{\text{inter}}_k(t)$, and $Q_k(t)$ for each queue k. To prove $\mathbf{Q}(t)$, the vector of actual queue lengths, can be stabilized, we will show that both $Q^{\text{inter}}_k(t)$ and $|Q_k(t) - Q^{\text{inter}}_k(t)|$ can be mean-rate stabilized by $\mathsf{SCH}_{\text{avg}}$ for all k. Since the summation of mean-rate stable random processes is still mean-rate stable, $\mathbf{Q}(t)$ can thus be mean-rate stabilized by $\mathsf{SCH}_{\text{avg}}$.

With the above road map, we now specify the update rules for $q^{\text{inter}}_k(t)$ and $Q^{\text{inter}}_k(t)$. Initially, $q^{\text{inter}}_k(1)$ and $Q^{\text{inter}}_k(1)$ are set to 0 for all k. In the end of each time t, we compute $\mathbf{q}^{\text{inter}}(t+1)$ using the preferred schedule $\mathbf{x}^*(t)$ chosen by $\mathsf{SCH}_{\text{avg}}$:

$$\begin{aligned}\mathbf{q}^{\text{inter}}(t+1) =& \mathbf{q}^{\text{inter}}(t) + \mathcal{A}\cdot\mathbf{a}(t)\\ &+ \left(\mathcal{B}^{\text{out}}(\mathsf{cq}(t)) - \mathcal{B}^{\text{in}}(\mathsf{cq}(t))\right)\cdot\mathbf{x}^*(t).\end{aligned} \tag{9}$$

Comparing (9) and (7), we can see that $\mathbf{q}^{\text{inter}}(t)$ is updated by the *realization* of the input/output service matrices while $\mathbf{q}(t)$ is updated by the *expected* input/output service matrices.

We can rewrite (9) in the following equivalent form:

$$q^{\text{inter}}_k(t+1) = q^{\text{inter}}_k(t) - \mu_{\text{out},k}(t) + \mu_{\text{in},k}(t),\ \forall k, \tag{10}$$

[5] Sometimes we may not be able to execute/schedule the preferred service activities chosen by (5). This is the reason why we only call the $\mathbf{x}^*(t)$ vector in (5) a preferred choice, instead of a scheduling choice.

[6] The reason of letting the system idle is to facilitate rigorous stability analysis. In practice, when the preferred choice is infeasible, we can choose a feasible SA n with the largest back-pressure computed by the actual queue lengths $Q_k(t)$ instead of the virtual queue lengths $q_k(t)$.

[7] $q^{\text{inter}}_k(t)$ and $Q^{\text{inter}}_k(t)$ are used only for the proof and are not needed when running the scheduling algorithm.

where

$$\mu_{\text{out},k}(t) = \sum_{n=1}^{N} \left(\beta^{\text{in}}_{k,n}(\mathsf{cq}(t)) \cdot x^*_n(t)\right), \tag{11}$$

$$\mu_{\text{in},k}(t) = \sum_{m=1}^{M} \left(\alpha_{k,m} \cdot a_m(t)\right) + \sum_{n=1}^{N} \left(\beta^{\text{out}}_{k,n}(\mathsf{cq}(t)) \cdot x^*_n(t)\right). \tag{12}$$

Here, $\mu_{\text{out},k}$ is the amount of packets coming "out of queue k", which is decided by the "input rates of SA n". Similarly, $\mu_{\text{in},k}$ is the amount of packets "entering queue k", which is decided by the "output rates of SA n" and the packet arrival rates. We now update $\mathbf{Q}^{\text{inter}}(t+1)$ by

$$Q^{\text{inter}}_k(t+1) = \left(Q^{\text{inter}}_k(t) - \mu_{\text{out},k}(t)\right)^+ + \mu_{\text{in},k}(t), \ \forall k, \tag{13}$$

where $(v)^+ = \max\{0, v\}$.

The difference between $q^{\text{inter}}_k(t)$ and $Q^{\text{inter}}_k(t)$ is that the former can be still be strictly negative when updated via (10) while we enforce the latter to be non-negative.

To compare $Q^{\text{inter}}_k(t)$ and $Q_k(t)$, we observe that by (13), $Q^{\text{inter}}_k(t)$ is updated by the preferred service vector $\mathbf{x}^*(t)$ without considering whether the preferred SA n^* is feasible or not. In contrast, the update rule of the actual queue length $Q_k(t)$ is quite different. For example, if SA n^* is infeasible, then the system remains idle and we have

$$Q_k(t+1) = Q_k(t) + \sum_{m=1}^{M} \left(\alpha_{k,m} \cdot a_m(t)\right). \tag{14}$$

Note that (14) differs significantly from (13). For example, say we have $Q_k(t) = 0$ to begin with. When SA n^* is infeasible, by (14) the aggregate increase of $Q_k(t)$ depends only on the new packet arrivals. But the aggregate increase of $Q^{\text{inter}}_k(t)$, assuming $Q^{\text{inter}}_k(t) = 0$, depends on the service rates of the preferred $x^*_n(t)$ as well,[8] see the two terms in (12).

We first focus on the absolute difference $|Q_k(t) - Q^{\text{inter}}_k(t)|$. We use $n(t)$ to denote the preferred SA suggested by the back-pressure scheduler in (5) and (6). We now define an event, which is called the *null activity* of queue k at time t. We say the null activity occurs at queue k if (i) $k \in \mathcal{I}_{n(t)}$ and (ii) $Q^{\text{inter}}_k(t) < \beta^{\text{in}}_{k,n(t)}(\mathsf{cq}(t))$. That is, the null activity describes the event that the preferred SA shall consume the packets in queue k (since $k \in \mathcal{I}_{n(t)}$) but at the same time $Q^{\text{inter}}_k(t) < \beta^{\text{in}}_{k,n}(\mathsf{cq}(t))$. Note that the null activity is defined based on comparing the intermediate actual queue length $Q^{\text{inter}}_k(t)$ and the actual realization of the packet consumption $\beta^{\text{in}}_{k,n(t)}(\mathsf{cq}(t))$. For comparison, whether the SA $n(t)$ is feasible depends on whether the actual queue length $Q_k(t)$ is larger or less than 1. Therefore the null activities are not directly related to the event that SA $n(t)$ is infeasible.[9]

Let $N_{\mathsf{NA},k}(t)$ be the aggregate number of null activities occurred at queue k up to time t. That is,

$$N_{\mathsf{NA},k}(t) \triangleq \sum_{\tau=1}^{t} I(k \in \mathcal{I}_{n(\tau)}) \cdot I(Q^{\text{inter}}_k(\tau) < \beta^{\text{in}}_{k,n(\tau)}(\mathsf{cq}(\tau)))$$

where $I(\cdot)$ is the indicator function. We then have

Lemma 2: For all $k = 1, 2, \cdots, K$, there exist K non-negative coefficients $\gamma_1, ..., \gamma_K$ such that

$$\mathsf{E}\left(|Q_k(t) - Q^{\text{inter}}_k(t)|\right) \le \sum_{\tilde{k}=1}^{K} \gamma_{\tilde{k}} \mathsf{E}\left(N_{\mathsf{NA},\tilde{k}}(t)\right). \tag{15}$$

for all $t = 1$ to ∞.

The proof of Lemma 2 is relegated to Appendix A of [21]. In Appendix D of [21], we prove that $Q^{\text{inter}}_k(t)$ and $N_{\mathsf{NA},k}(t)$ can be mean-rate stabilized by $\mathsf{SCH}_{\text{avg}}$ for all k. Therefore, by Lemma 2, $|Q_k(t) - Q^{\text{inter}}_k(t)|$ can be mean-rate stabilized and so can $Q_k(t)$. Proposition 3 is thus proven.

V. The Combined Dynamic INC Solution

We now combine the discussions in Sections III and IV. As discussed in Section III, the 7 INC operations form a vr-network as described in Fig. 4. How s generates an NC packet is now converted to a scheduling problem of the vr-network of Fig. 4, which has $K = 5$ queues, $M = 2$ IAs, and $N = 7$ SAs. The 5-by-2 input matrix $\mathcal{A}$ contains 2 ones, since the packets arrive at either $Q^1_\emptyset$ or $Q^2_\emptyset$. Given the channel quality $\mathsf{cq}(t) = c$, the expected input / output service matrices $\overline{\mathcal{B}^{\text{in}}(c)}$ and $\overline{\mathcal{B}^{\text{out}}(c)}$ can be derived from Table II.

For illustration, suppose that $\mathsf{cq}(t)$ is Bernoulli with parameter $1/2$ (i.e., flipping a perfect coin and the relative frequency $f_0 = f_1 = 0.5$). Also suppose that when $\mathsf{cq}(t) = 0$, with probability 0.5 (resp. 0.7) d_1 (resp. d_2) can successfully receive a packet transmitted by s; and when $\mathsf{cq}(t) = 1$, with probability $2/3$ (resp. $1/3$) d_1 (resp. d_2) can successfully receive a packet transmitted by s. Further assume that all the success events of d_1 and d_2 are independent. If we order the 5 queues as $\left[\mathbf{Q}^1_\emptyset, \mathbf{Q}^2_\emptyset, \mathbf{Q}^1_{\{2\}}, \mathbf{Q}^2_{\{1\}}, \mathbf{Q}_{\text{mix}}\right]$, the 7 service activities as $[\text{NC1}, \text{NC2}, \text{DX1}, \text{DX2}, \text{PM}, \text{RC}, \text{CX}]$, then the matrices of

[8] In the original DMW algorithm [16], the quantity "actual queue length" is updated by (13) instead of (14). The "actual queue lengths in [16]" thus refer to the register value $Q^{\text{inter}}_k(t)$ rather than the number of physical packets in the buffer/queue. In this work, we rectify this inconsistency by renaming "the actual queue lengths in [16]" the "intermediate actual queue lengths $Q^{\text{inter}}_k(t)$."

[9] If $Q^{\text{inter}}_k(t) \ge Q_k(t)$ for all k and t with probability 1, then the event "SA $n(t)$ is infeasible" implies the null activity for at least one of the input queues of SA $n(t)$. One can then upper bound the frequency of SA $n(t)$ being infeasible by upper bounding how frequently we encounter the null activities of queue k as suggested in [16]. Unfortunately, we have proven that $Q^{\text{inter}}_k(t) < Q_k(t)$ with strictly positive probability for some k and t. The arguments in [16] thus do not hold. Instead, we introduce a new *expectation-based* dominance relationship in Lemma 2 and use it to establish the connection between null activities and the instants SA $n(t)$ is infeasible. Also see [21].

the SPN become

$$\mathcal{A} = \begin{bmatrix} 1 & 0 & 0 & 0 & 0 \\ 0 & 1 & 0 & 0 & 0 \end{bmatrix}^{\mathsf{T}},$$

$$\overline{\mathcal{B}^{\text{in}}(0)} = \begin{bmatrix} 0.85 & 0 & 0 & 0 & 0.85 & 0 & 0 \\ 0 & 0.85 & 0 & 0 & 0.85 & 0 & 0 \\ 0 & 0 & 0.5 & 0 & 0 & 0 & 0.5 \\ 0 & 0 & 0 & 0.7 & 0 & 0 & 0.7 \\ 0 & 0 & 0 & 0 & 0 & 0.85 & 0 \end{bmatrix},$$

$$\overline{\mathcal{B}^{\text{in}}(1)} = \begin{bmatrix} 7/9 & 0 & 0 & 0 & 7/9 & 0 & 0 \\ 0 & 7/9 & 0 & 0 & 7/9 & 0 & 0 \\ 0 & 0 & 2/3 & 0 & 0 & 0 & 2/3 \\ 0 & 0 & 0 & 1/3 & 0 & 0 & 1/3 \\ 0 & 0 & 0 & 0 & 0 & 7/9 & 0 \end{bmatrix},$$

$$\overline{\mathcal{B}^{\text{out}}(0)} = \begin{bmatrix} 0 & 0 & 0 & 0 & 0 & 0 & 0 \\ 0 & 0 & 0 & 0 & 0 & 0 & 0 \\ 0.35 & 0 & 0 & 0 & 0 & 0.35 & 0 \\ 0 & 0.15 & 0 & 0 & 0 & 0.15 & 0 \\ 0 & 0 & 0 & 0 & 0.85 & 0 & 0 \end{bmatrix},$$

$$\overline{\mathcal{B}^{\text{out}}(1)} = \begin{bmatrix} 0 & 0 & 0 & 0 & 0 & 0 & 0 \\ 0 & 0 & 0 & 0 & 0 & 0 & 0 \\ 1/9 & 0 & 0 & 0 & 0 & 1/9 & 0 \\ 0 & 4/9 & 0 & 0 & 0 & 4/9 & 0 \\ 0 & 0 & 0 & 0 & 7/9 & 0 & 0 \end{bmatrix}.$$

For example, the seventh column of $\overline{\mathcal{B}^{\text{in}}(0)}$ indicates that when $\mathsf{cq}(t) = 0$ and CLASSIC-XOR is activated, with probability 0.5 (resp. 0.7) 1 packet will be consumed from queue $\mathbf{Q}^1_{\{2\}}$ (resp. $\mathbf{Q}^2_{\{1\}}$). The third row of $\overline{\mathcal{B}^{\text{out}}(1)}$ indicates that when $\mathsf{cq}(t) = 1$, queue $\mathbf{Q}^1_{\{2\}}$ will increase by 1 with probability 1/9 (resp. 1/9) if NON-CODING-1 (resp. REACTIVE-CODING) is activated since it corresponds to the event that d_1 receives the transmitted packet but d_2 does not.

We can now use the proposed DMW scheduler in (5), (6), and (7) to compute the preferred scheduling decision in every time t. We activate the preferred decision if it is feasible. If not, then the system remains idle.

For general channel parameters (including but not limited to this simple example), after computing the $\overline{\mathcal{B}^{\text{in}}(c)}$ and $\overline{\mathcal{B}^{\text{out}}(c)}$ of the vr-network in Fig. 4 with the help of Table II, we can explicitly compare the mean-rate stability region in Propositions 2 and 3 with the Shannon capacity region in [15]. In the end, we have the following proposition.

Proposition 4: The mean-rate stability region of the proposed INC-plus-SPN-scheduling scheme always matches the block-code capacity of time-varying channels.

A detailed proof of Proposition 4 is provided in Appendix E of the technical report [21].

Remark: During numerical simulations, we notice that we can further revise the proposed scheme to reduce the actual queue lengths $Q_k(t)$ by $\approx 50\%$ even though we do not have any rigorous proofs/performance guarantees for the revised scheme. That is, when making the scheduling decision by (5), we can compute $\mathbf{d}(t)$ by

$$\mathbf{d}(t) = \left(\overline{\mathcal{B}^{\text{in}}(\mathsf{cq}(t))} - \overline{\mathcal{B}^{\text{out}}(\mathsf{cq}(t))}\right)^{\mathsf{T}} \mathbf{q}^{\text{inter}}(t) \qquad (16)$$

where $\mathbf{q}^{\text{inter}}(t)$ is the intermediate virtual queue length defined in (10). The intuition behind is that the new back-pressure in (16) allows the scheme to directly control $q_k^{\text{inter}}(t)$, which, when compared to the virtual queue $\mathbf{q}(t)$ in (7), is more closely related to the actual queue length[10] $Q_k(t)$.

A. Extensions For Rate Adaption

The proposed dynamic INC solution can be generalized for rate adaptation, also known as adaptive coding and modulation. For illustration, we consider the following example.

Consider 2 possible error correcting rates (1/2 and 3/4); 2 possible modulation schemes QPSK and 16QAM; and jointly there are 4 possible combinations. The lowest throughput combination is rate-1/2 plus QPSK and the highest throughput combination is rate-3/4 plus 16QAM. Assuming the packet size is fixed. If the highest throughput combination takes 1-unit time to finish sending 1 packet, then the lowest throughput combination will take 3-unit time. For these 4 possible (rate,modulation) combinations, we denote the unit-time to finish transmitting 1 packet as T_1 to T_4, respectively.

For the i-th (rate,modulation) combination, $i = 1$ to 4, source s can measure the probability that d_1 and/or d_2 successfully hears the transmission, and denote the corresponding probability vector by $\vec{p}^{(i)}$. Source s then uses $\vec{p}^{(i)}$ to compute the $\overline{\mathcal{B}^{\text{in},(i)}(c)}$ and $\overline{\mathcal{B}^{\text{out},(i)}(c)}$ for the vr-network when $\mathsf{cq}(t) = c$. At any time t, after observing $\mathsf{cq}(t)$ source s computes the back-pressure by

$$\mathbf{d}^{(i)}(t) = \left(\overline{\mathcal{B}^{\text{in},(i)}(\mathsf{cq}(t))} - \overline{\mathcal{B}^{\text{out},(i)}(\mathsf{cq}(t))}\right)^{\mathsf{T}} \mathbf{q}(t).$$

We can now compute the preferred scheduling choice by

$$\underset{i\in\{1,2,3,4\},\mathbf{x}\in\mathfrak{X}}{\arg\max} \frac{\mathbf{d}^{(i)}(t)^{\mathsf{T}} \cdot \mathbf{x}}{T_i} \qquad (17)$$

and update the virtual queue length $\mathbf{q}(t)$ by (7). Namely, the back-pressure $\mathbf{d}^{(i)}(t)^{\mathsf{T}} \cdot \mathbf{x}$ is scaled inverse proportionally with respect to T_i, the time it takes to finish the transmission of 1 packet. If the preferred SA n^* is feasible, then we use the i^*-th (rate,modulation) combination plus the coding choice n^* for the current transmission. If the preferred SA n^* is infeasible, then we let the system remain idle.

One can see that the new scheduler (17) automatically balances the packet reception status (the $\mathbf{q}(t)$ terms), the success overhearing probability of different (rate,modulation) (the $\overline{\mathcal{B}^{\text{in},(i)}(\mathsf{cq}(t))}$ and $\overline{\mathcal{B}^{\text{out},(i)}(\mathsf{cq}(t))}$ terms), and different amount of time it takes to finish transmission of a coded/uncoded packet (the T_i term). In all the numerical experiments we have performed, the new scheduler (17) robustly achieves the optimal throughput with adaptive coding and modulation.

B. Practical Issues

In addition to the theoretic focus of this work, here we discuss two practical issues of the proposed solution.

Delayed Feedback: In this work, we assume that the ACK feedback is transmitted via a separate, error-free control channel *immediately after* each forward packet transmission. The

[10]There are four types of queue lengths in this work: $\mathbf{q}(t)$, $\mathbf{q}^{\text{inter}}(t)$, $\mathbf{Q}^{\text{inter}}(t)$, and $\mathbf{Q}(t)$ and they range from the most artificially-derived $\mathbf{q}(t)$ to the most realistic metric, the actual queue length $\mathbf{Q}(t)$.

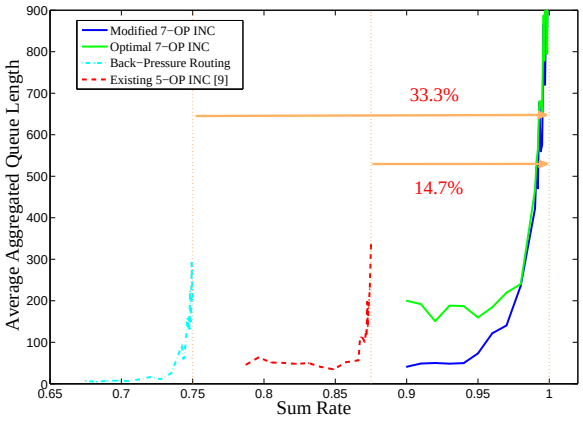

Fig. 5. The backlog of four different schemes for a time-varying channel with $\mathsf{cq}(t)$ uniformly distributed on $\{1,2\}$, and the packet delivery probability being $\vec{p}=(0,0.5,0.5,0)$ if $\mathsf{cq}(t)=1$ and $\vec{p}=(0,0,0,1)$ if $\mathsf{cq}(t)=2$.

error-free assumption is justified by the fact that in practice, ACK is usually transmitted through the lowest MCS level to ensure the most reliable transmission.

On the other hand, the instant feedback assumption may not hold in practice since delayed feedback mechanisms are used widely in real-world systems in order to minimize the number of transmission-reception transition intervals. For example, the mandatory Block-ACK mechanism in IEEE 802.11n standard forces the feedbacks to be aggregated and to be transmitted at the end of each Transmit Opportunity (TXOP) at once, instead of after reception of each packet.

Our proposed solution can be modified to accommodate the delayed feedback by incorporating the designs in [23]. The main idea of [23] is to pipelining the operations and let the base-station only processes those *properly acknowledged* packets. This converts the delayed feedback scenario to an equivalent instant feedback set-up. See [23] for detailed discussion on handling delayed feedback.

Scability: Although the discussion of this work focuses exclusively on the 2-client case, there are many possible ways of extending the solution to more-than-2-client applications.[11] For example, the router of city-WiFi may serve multiple smart devices and laptops, and suppose we have 10 clients. Before transmission, we can first estimate how much throughput gain we can have if we group any two specific clients as a pair and perform INC on this pair. Then, we divide the clients into 5 pairs of clients that can lead to the highest throughput gain. After dividing the clients into pairs, we start the packet transmission and apply the dynamic INC solution within each pair. The detailed implementation of such an approach is beyond the scope of this work.

VI. Simulation Results

We simulate the proposed optimal 7-operation INC + scheduling solution and compare the results with the existing INC solutions and the (back-pressure) pure-routing solutions. We use a custom built simulator in MATLAB. Even though we spent a quite amount of effort/pages on proving the correctness, the core algorithm is pretty simple and could be implemented in less than 200 lines of codes to compute the chosen coding operation at each iteration.

In Fig. 5, we simulate a simple time-varying channel situation first described in Section III-A. Specifically, the channel quality $\mathsf{cq}(t)$ is i.i.d. distributed and for any t, $\mathsf{cq}(t)$ is uniformly distributed on $\{1,2\}$. When $\mathsf{cq}(t)=1$, the success probabilities are $\vec{p}^{(1)}=(0,0.5,0.5,0)$ and when $\mathsf{cq}(t)=2$, the success probabilities are $\vec{p}^{(2)}=(0,0,0,1)$, respectively. We consider four different schemes: (i) Back-pressure (BP) + pure routing; (ii) BP + INC with 5 operations [10]; (iii) The proposed DMW+INC with 7 operations, and (iv) The modified DMW+INC with 7 operations that use $q_k^{\text{inter}}(t)$ to compute the back pressure, see (16), instead of $q_k(t)$ in (6).

We choose perfectly fair $(R_1,R_2)=(\theta,\theta)$ and gradually increase the θ value and plot the stability region. For each experiment, i.e., each θ, we run the schemes for 10^5 time slots. The horizontal axis is the sum rate $R_1+R_2=2\theta$ and the vertical axis is the aggregate backlog (averaged over 10 trials) in the end of 10^5 slots. By [15], the sum rate Shannon capacity is 1 packet/slot, the best possible rate for 5-OP INC is 0.875 packet/slot, and the best pure routing rate is 0.75 packet/slot, which are plotted as vertical lines in Fig. 5. The simulation results confirm our analysis. The proposed 7-operation dynamic INC has a stability region matching the Shannon block code capacity and provides 14.7% throughput improvement over the 5-operation INC, and 33.3% over the pure-routing solution.

Also, both our original proposed solution (using $q_k(t)$) and the modified solution (using $q_k^{\text{inter}}(t)$) can approach the stability region while the modified solution has smaller backlog. This phenomenon is observed throughout all our experiments. As a result, in the following experiments, we only report the results of the modified solution.

Next we simulate the scenario of 4 different channel qualities: $\mathsf{CQ}=\{1,2,3,4\}$. The varying channel qualities could model the situations like the different packet transmission rates and loss rates due to time-varying interference caused by the primary traffic in a cognitive radio environment. We assume four possible channel qualities with the corresponding probability distributions being $\vec{p}^{(1)}=(p^{(1)}_{\overline{d_1d_2}},p^{(1)}_{d_1\overline{d_2}},p^{(1)}_{\overline{d_1d_2}},p^{(1)}_{d_1d_2})=(0.14,0.06,0.56,0.24)$, $\vec{p}^{(2)}=(0.14,0.56,0.06,0.24)$, $\vec{p}^{(3)}=(0.04,0.16,0.16,0.64)$, and $\vec{p}^{(4)}=(0.49,0.21,0.21,0.09)$ in both Figs. 6(a) and 6(b). The difference is that in Fig. 6(a), the channel quality $\mathsf{cq}(t)$ is i.i.d. with probability (f_1,f_2,f_3,f_4) being $(0.15,0.15,0.35,0.35)$. In Fig. 6(b) the $\mathsf{cq}(t)$ is i.i.d. but with different frequency $(f_1,f_2,f_3,f_4)=(0.25,0.25,0.25,0.25)$. In Fig. 6(c), we consider the same set of channel qualities but choose $\mathsf{cq}(t)$ to be periodic with period 12 and the first period being $1,1,1,2,2,2,3,3,3,4,4,4$. This scenario can be considered as an exmple of the Markovian channel quality. Again, we assume perfect fairness $(R_1,R_2)=(\theta,\theta)$. The sum-rate Shannon capacity is $R_1+R_2=0.716$ when $(f_1,f_2,f_3,f_4)=(0.15,0.15,0.35,0.35)$ and $R_1+R_2=$

[11] Unfortunately, we can no longer guarantee the optimality of the dynamic INC solution. This is because even the block-code capacity (Shannon capacity) for more than 3-client case remains largely unknown [7].

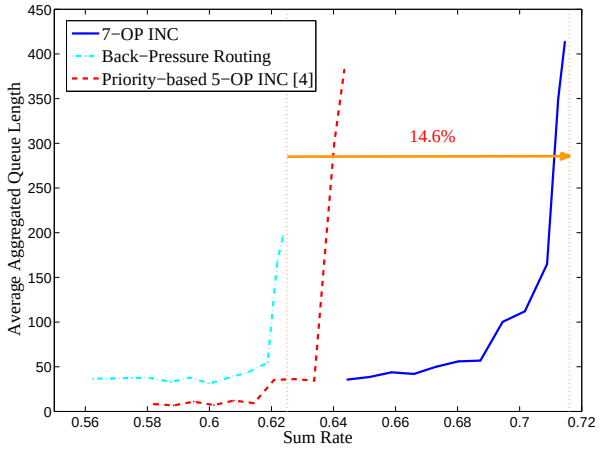

(a) $(f_1, f_2, f_3, f_4) = (0.15, 0.15, 0.35, 0.35)$.

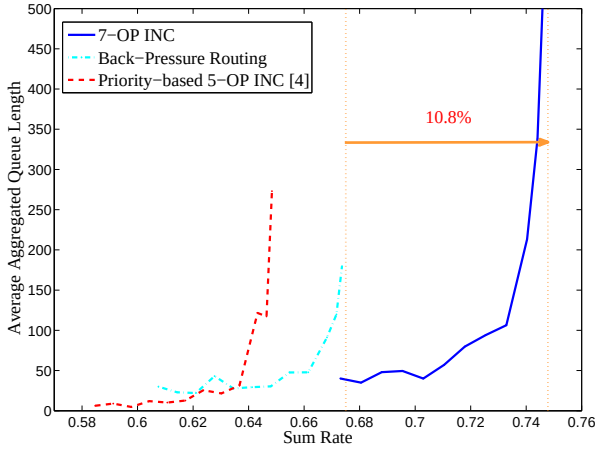

(b) $(f_1, f_2, f_3, f_4) = (0.25, 0.25, 0.25, 0.25)$.

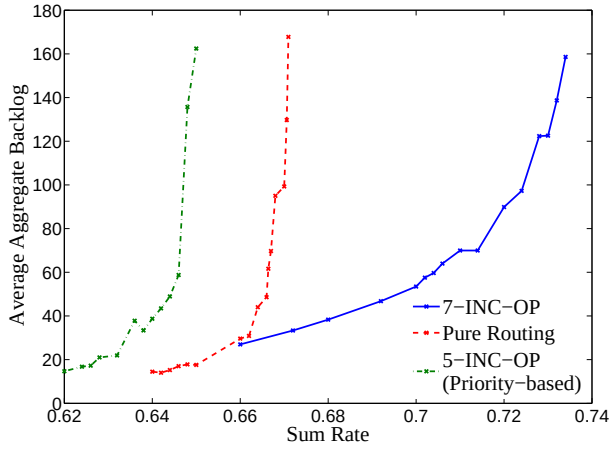

(c) Periodic channel quality with 3-repetition.

Fig. 6. The backlog comparison with $\mathsf{cq}(t)$ chosen from $\{1, 2, 3, 4\}$ and $\vec{p}^{(1)} = (0.14, 0.06, 0.56, 0.24)$, $\vec{p}^{(2)} = (0.14, 0.56, 0.06, 0.24)$, $\vec{p}^{(3)} = (0.04, 0.16, 0.16, 0.64)$, and $\vec{p}^{(4)} = (0.49, 0.21, 0.21, 0.09)$.

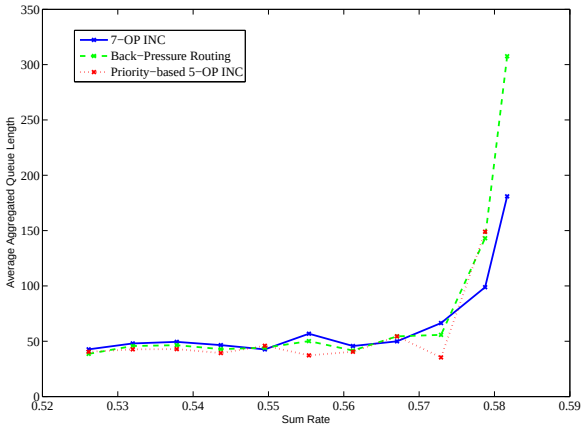

Fig. 7. $(f_1, f_2, f_3, f_4) = (0.25, 0.25, 0.25, 0.25)$ with $R_1 = 10 \cdot R_2$. The backlog comparison with $\mathsf{cq}(t)$ chosen from $\{1, 2, 3, 4\}$ and $\vec{p}^{(1)} = (0.14, 0.06, 0.56, 0.24)$, $\vec{p}^{(2)} = (0.14, 0.56, 0.06, 0.24)$, $\vec{p}^{(3)} = (0.04, 0.16, 0.16, 0.64)$, and $\vec{p}^{(4)} = (0.49, 0.21, 0.21, 0.09)$.

TABLE III
SIMULATIONS FOR THE SETTINGS IN FIGS. 5 AND 6 AT DIFFERENT ARRIVAL RATES. THE REPRESENTATION $(x; y)$ MEANS THAT x (RESP. y) IS FOR 90% (RESP. 95%) OF THE OPTIMAL PACKET ARRIVAL RATE.

	Avg. end-to-end delay (time slot)	Avg. receiver buffer size (no. of packets)	Avg. receiver buffer size of existing solutions
Fig. 5	(34,84; 85.20)	(7.35; 17.94)	(28.74; 128.20)
Fig. 6(a)	(33.41; 72.03)	(5.19; 12.45)	(14.20; 39.34)
Fig. 6(b)	(37.56; 75.23)	(6.20; 13.62)	(16.94; 41.66)

0.748 when $(f_1, f_2, f_3, f_4) = (0.25, 0.25, 0.25, 0.25)$, and the pure routing sum-rate capacity is $R_1 + R_2 = 0.625$ when $(f_1, f_2, f_3, f_4) = (0.15, 0.15, 0.35, 0.35)$ and $R_1 + R_2 = 0.675$ when $(f_1, f_2, f_3, f_4) = (0.25, 0.25, 0.25, 0.25)$. We simulate our modified 7-OP INC, the priority-based solution in [6], and a standard back-pressure routing scheme [14].

Although the priority-based scheduling solution is provably optimal for fixed channel quality, it is less robust and can sometimes be substantially suboptimal (see Fig. 6(b)) due to the ad-hoc nature of the priority-based policy. For example, as depicted by Figs. 6(a) and 6(b), the pure-routing solution outperforms the 5-operation scheme for one set of frequency (f_1, f_2, f_3, f_4) while the order is reversed for another set of frequency. On the other hand, the proposed 7-operation scheme consistently outperforms all the existing solutions and has a stabiliby region matching the Shannon block-code capacity. We have tried many other combinations of time-varying channels. In all our simulations, the proposed DMW scheme always achieves the block-code capacity in [15] and outperforms routing and any existing solutions [6], [10]. Fig. 7 demonstrates the aggregated backlog result under a scenario that is similar to Fig. 6(b) but with an extremely uneven arrival rate pair, $R_1 = 10 \cdot R_2$. In this case, the network coding-based solution can barely provide significant throughput gain as proven in [15].

Using the same settings as in Figs. 5, 6(a), and 6(b), Table III examines the corresponding end-to-end delay and

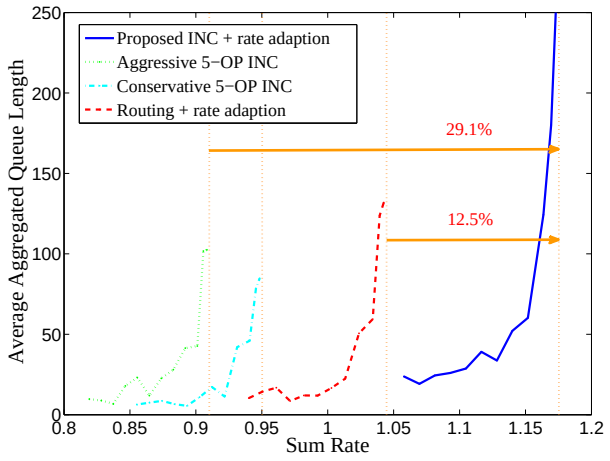

Fig. 8. The backlog of four different schemes for rate adaptation with two possible (error-correcting-code rate,modulation) combinations. The back-pressure-based INC scheme in [10] is used in both aggressive and conservative 5-OP INC, where the former always chooses the high-throughput (rate,modulation) combination while the latter always chooses the low-throughput (rate,modulation) combination.

buffer usage. Specifically the end-to-end delay measures the time slots each packet takes from its arrival at s to the time slot it is successfully decoded by its intended destination, which includes the queueing, propagation, and decoding delay. The buffer size is measured at the receivers according to our buffer management policy in Section III-C. The statistics are derived under either 90% or 95% of the optimal sum arrival rate, which corresponds to 0.9 or 0.95 packets/slot; 0.64 or 0.68 packets/slot; and 0.67 or 0.71 packets/slot for the settings in Figs. 5, 6(a), and 6(b), respectively. The last column of Table III also reports the buffer usage if we use the existing (i^*, j^*)-based buffer pruning policy described in Section III-C.

We notice that our scheme has small delay and buffer usage at 90% of the optimal arrival rate and the delay and buffer size are still quite manageable even at 95% of the optimal arrival rate. It is worth noting that 4 out of the 6 chosen arrival rates are beyond the stability region of the best existing routing/NC solutions [6], [9], [10] and those schemes will thus have exploding delay and buffer sizes under those cases. Table III also confirms that the solution proposed in Section III-C can significantly reduce the buffer size of the existing NC solutions [5], [6], [9], [10].

Our solution in Section V-A is the first dynamic INC design that achieves the optimal linear INC capacity with rate-adaptation [15]. Fig. 8 compares its performance with existing routing-based rate-adaptation scheme and the existing INC schemes, the latter of which are designed without rate adaptation. We assume there are two available (error-correcting-code rate,modulation) combinations; and the first (resp. second) combination takes 1 second (resp. $\frac{1}{3}$ second) to finish transmitting a single packet. I.e., the transmission rate of the second combination is 3 times faster.

We further assume the packet delivery probability is $\vec{p} = (p_{\overline{d_1}\overline{d_2}}, p_{d_1\overline{d_2}}, p_{\overline{d_1}d_2}, p_{d_1d_2}) = (0.005, 0.095, 0.045, 0.855)$ if the first combination is selected and $\vec{p} = (0.48, 0.32, 0.12, 0.08)$ for the second combination. That is, the low-throughput combination is likely to be overheard by both destinations and the high-throughput combination has a much lower success probability. We can compute the corresponding Shannon capacity by modifying the equations in [15]. We then use the proportional fairness objective function $\xi(R_1, R_2) = \log(R_1) + \log(R_2)$ and find the maximizing R_1^* and R_2^* over the Shannon capacity region, which are $(R_1^*, R_2^*) = (0.6508, 0.5245)$ packets per second.

After computing (R_1^*, R_2^*), we assume the following dynamic packet arrivals. We define $(R_1, R_2) = \theta \cdot (R_1^*, R_2^*)$ for any given $\theta \in (0, 1)$. For any experiment (i.e., for any given θ), the arrivals of session-i packets is a Poisson random process with rate R_i packets per second for $i = 1, 2$.

Each point of the curves of Fig. 8 consists of 10 trials and each trial lasts for 10^5 seconds. We compare the performance of our scheme in Section V-A with (i) Pure-routing with rate-adaptation; (ii) aggressive 5-OP INC, i.e., use the scheme in [10] and always choose combination 2; and (iii) conservative 5-OP INC, i.e., use the scheme in [10] and always choose combination 1. We also plot the optimal routing-based rate-adaptation rate and the optimal Shannon-block-code capacity rate as vertical lines.

Since our proposed scheme jointly decides which (rate,modulation) combination and which INC operation to use in an optimal way, see (17), the stability region of our scheme matches the Shannon capacity with rate-adaptation. It provides 12.51% throughput improvement over the purely routing-based rate-adaptation solution, see Fig. 8.

Furthermore, if we perform INC but always choose the low-throughput (rate,modulation), as suggested in some existing works [24], then the largest sum-rate $R_1 + R_2 = \theta^*_{\text{cnsv. 5-OP}}(R_1^* + R_2^*) = 0.9503$, which is worse than pure routing with rate-adaptation $\theta^*_{\text{routing,RA}}(R_1^* + R_2^*) = 1.0446$. Even if we always choose the high-throughput (rate,modulation) with 5-OP INC, then the largest sum-rate $R_1 + R_2 = \theta^*_{\text{aggr. 5-OP}}(R_1^* + R_2^*) = 0.9102$ is even worse than the conservative 5-OP INC capacity. We have tried many other rate-adaptation scenarios. In all our simulations, the proposed DMW scheme always achieves the capacity and outperforms pure-routing, conservative 5-OP INC, and aggressive 5-OP INC.

It is worth emphasizing that in our simulation, for any fixed (rate,modulation) combination, the channel quality is also fixed. Therefore since 5-OP scheme is throughput optimal for fixed channel quality [11], it is guaranteed that the 5-OP scheme is throughput optimal when using a fixed (rate,modulation) combination. Our results thus show that using a fixed (rate,modulation) combination is the main reason of the suboptimal performance. At the same time, the proposed scheme in (5), (7), and (17) can dynamically decide which (rate,modulation) combination to use for each transmission and achieve the largest possible stability region.

VII. Conclusion

We have proposed a new 7-operation INC scheme together with the corresponding scheduling algorithm to achieve the optimal downlink throughput of the 2-flow access point network

with time varying channels. Based on binary XOR operations, the proposed solution admits ultra-low encoding/decoding complexity with efficient buffer management and minimal communication and control overhead. The proposed algorithm has also been generalized for rate adaptation and it again robustly achieves the optimal throughput in all the numerical experiments. A byproduct of this paper is a throughput-optimal scheduling solution for SPNs with random departure, which could further broaden the applications of SPNs to other real-world applications.

REFERENCES

[1] S.-Y. Li, R. Yeung, and N. Cai, "Linear network coding," *IEEE Trans. Inf. Theory*, vol. 49, no. 2, pp. 371–381, Feb 2003.

[2] T. Ho and H. Viswanathan, "Dynamic algorithms for multicast with intra-session network coding," *Information Theory, IEEE Transactions on*, vol. 55, no. 2, pp. 797–815, 2009.

[3] A. Khreishah, C.-C. Wang, and N. Shroff, "Rate control with pairwise intersession network coding," *Networking, IEEE/ACM Transactions on*, vol. 18, no. 3, pp. 816–829, June 2010.

[4] C.-C. Wang and N. Shroff, "Pairwise intersession network coding on directed networks," *Information Theory, IEEE Transactions on*, vol. 56, no. 8, pp. 3879–3900, Aug 2010.

[5] S. Katti, H. Rahul, W. Hu, D. Katabi, M. Médard, and J. Crowcroft, "XORs in the air: Practical wireless network," in *Proc. ACM Special Interest Group on Data Commun. (SIGCOMM)*, 2006.

[6] Y. Sagduyu, L. Georgiadis, L. Tassiulas, and A. Ephremides, "Capacity and stable throughput regions for the broadcast erasure channel with feedback: An unusual union," *Information Theory, IEEE Transactions on*, vol. 59, no. 5, pp. 2841–2862, 2013.

[7] C.-C. Wang, "On the capacity of 1-to-K broadcast packet erasure channels with channel output feedback," *IEEE Trans. Inf. Theory*, vol. 58, no. 2, pp. 931–956, Feb 2012.

[8] ——, "On the capacity of wireless 1-hop intersession network coding — a broadcast packet erasure channel approach," *IEEE Trans. on Information Theory*, vol. 58, no. 2, pp. 957–988, Feb 2012.

[9] G. Paschos, L. Georgiadis, and L. Tassiulas, "Scheduling with pairwise xoring of packets under statistical overhearing information and feedback," *Queueing Systems*, vol. 72, no. 3-4, pp. 361–395, 2012.

[10] S. A. Athanasiadou, M. Gatzianas, L. Georgiadis, and L. Tassiulas, "Stable and capacity achieving xor–based policies for the broadcast erasure channel with feedback," in *Information Theory Proceedings (ISIT), 2013 IEEE International Symposium on*. IEEE, 2013.

[11] L. Georgiadis and L. Tassiulas, "Broadcast erasure channel with feedback — capacity and algorithms," in *Proc. 5th Workshop on Network Coding, Theory, & Applications (NetCod)*, Lausanne, Switzerland, June 2009, pp. 54–61.

[12] S. Zhao and X. Lin, "On the design of scheduling algorithms for end-to-end backlog minimization in multi-hop wireless networks," in *INFOCOM, 2012 Proceedings IEEE*, March 2012, pp. 981–989.

[13] ——, "Rate-control and multi-channel scheduling for wireless live streaming with stringent deadlines," in *INFOCOM, 2014 Proceedings IEEE*, April 2014, pp. 1923–1931.

[14] L. Tassiulas and A. Ephremides, "Stability properties of constrained queueing systems and scheduling policies for maximum throughput in multihop radio networks," *Automatic Control, IEEE Transactions on*, vol. 37, no. 12, pp. 1936–1948, 1992.

[15] C.-C. Wang and J. Han, "The capacity region of 2-receiver multiple-input broadcast packet erasure channels with channel output feedback," *Information Theory, IEEE Transactions on*, vol. 60, no. 9, pp. 5597–5626, Sep. 2014.

[16] L. Jiang and J. Walrand, "Stable and utility-maximizing scheduling for stochastic processing networks," in *Communication, Control, and Computing, 2009. Allerton 2009. 47th Annual Allerton Conference on*. IEEE, 2009, pp. 1111–1119.

[17] L. Huang and M. J. Neely, "Utility optimal scheduling in processing networks," *Performance Evaluation*, vol. 68, no. 11, pp. 1002–1021, 2011.

[18] G. Paschos, C. Fragiadakis, L. Georgiadis, and L. Tassiulas, "Wireless network coding with partial overhearing information," in *INFOCOM, 2013 Proceedings IEEE*, April 2013, pp. 2337–2345.

[19] W.-C. Kuo and C.-C. Wang, "Two-flow capacity region of the cope principle for wireless butterfly networks with broadcast erasure channels," *Information Theory, IEEE Transactions on*, vol. 59, no. 11, pp. 7553–7575, Nov 2013.

[20] M. J. Neely, "Stability and probability 1 convergence for queueing networks via lyapunov optimization," *Journal of Applied Mathematics*, vol. 2012, no. 831909, p. 35, 2012.

[21] W.-C. Kuo and C.-C. Wang, "Robust and optimal opportunistic scheduling for downlink 2-flow network coding with varying channel quality and rate adaptation," ePrint at http://arxiv.org/abs/1410.1851, Purdue University, Tech. Rep. TR-ECE-14-08, Oct. 2014.

[22] C.-C. Wang, D. Koutsonikolas, Y. C. Hu, and N. Shroff, "Fec-based ap downlink transmission schemes for multiple flows: Combining the reliability and throughput enhancement of intra- and inter-flow coding," *Perform. Eval.*, vol. 68, no. 11, pp. 1118–1135, Nov. 2011.

[23] X. Li, C.-C. Wang, and X. Lin, "On the capacity of immediately-decodable coding schemes for wireless stored-video broadcast with hard deadline constraints," *Selected Areas in Communications, IEEE Journal on*, vol. 29, no. 5, pp. 1094–1105, May 2011.

[24] S. Rayanchu, S. Sen, J. Wu, S. Banerjee, and S. Sengupta, "Loss-aware network coding for unicast wireless sessions: Design, implementation, and performance evaluation," in *SIGMETRICS*. Annapolis, Maryland, USA, Jun. 2008.